Original Article

Histological and Biochemical Comparative Study Between the Effect of Quercetin and Topiramate on Induced Diabetic Peripheral Neuropathy in Adult Male Albino Rats

Mai Amin Al-Moatasem, Azza Saleh Moawad Embaby, Salwa Khaled Mostafa Ibrahim, Asmaa Mahmoud Mostafa and Fatma Elzahraa Mohamed Abdellatef

Department of Medical Histology & Cell Biology, Faculty of Medicine, Beni-Suef University, Egypt

ABSTRACT

Introduction: Diabetic peripheral neuropathy (DPN) is a prevalent consequence for diabetes mellitus, significantly attributing to risk of amputation and mortality, if untreated.

Aim of the Work: To emphasize the possible regenerative capacities of Quercetin and Topiramate against induced DPN in rat models.

Material and Methods: 50 adult male albino rats were allocated into; control group (n=10) and experimental (diabetic) group (n=40) injected once by alloxan (150mg /kg/i.p). After establishing the diabetic model, rats were subdivided equally into 4 subgroups. Diabetic group, Quercetin treated diabetic group received Quercetin (100mg/Kg), Topiramate treated diabetic group received Topiramate (30mg/kg), and Combined treatment diabetic group received both Quercetin and Topiramate. Treatments were given by gastric gavage for 4 weeks then the blood samples were biochemically tested. Sciatic nerves were harvested for structural, ultrastructural and immunohistochemical assessment. H & E and toluidine were used for histological analyses and immunohistochemistry for assessing Caspase-3 and S-100 expressions and electron microscopy for ultrastructural examination. Data were analysed using computer software for morphometrical and statistical analysis.

Results: The diabetic group showed a remarkable structural, biochemical and immunohistochemical changes. There was a significant decline in nerve fibres count with disturbed organization, abnormal myelin configurations, axonopathy and a significant increase and decrease in Caspase-3 and S-100 immunoreactivity. Quercetin and Topiramate treatments resulted in a partial improvement with comparable effect. Interestingly, combined therapy resulted in remarkable improvement.

Conclusion: Concomitant administration of Quercetin and Topiramate have a superior therapeutic effect in a modal of a diabetic neuropathy than using either agent.

Received: 21 April 2025, **Accepted:** 10 June 2025

Key Words: Diabetic neuropathy, quercetin, topiramate.

Corresponding Author: Salwa Khaled Mostafa Ibrahim, MSc, Department of Medical Histology & Cell Biology, Faculty of Medicine, Beni-Suef University, Egypt, **Tel.**: +20 11 4640 3219, **E-mail:** salwakhaled19@gmail.com

ISSN: 1110-0559, Vol. 48, No. 3

INTRODUCTION

Number of diabetic patients in the world is steadily growing year after year, proposed to reach 700 million by 2045[1]. The most encountered complication of diabetes mellitus (DM) is diabetic peripheral neuropathy (DPN) as 50% of the individuals with diabetes suffer from DPN over the time, so it can be considered as major public health burden[2].

Mechanisms underlying DPN are complicated as they involve several cellular pathways still not fully understood. However, among those different mechanisms, oxidative stress has the upper hand in the induction of diabetic neuropathy, ending with the neuropathic pain[3].

In spite of the severe consequences of diabetic neuropathy, still there is no fundamental therapeutic regimen for DPN currently available[4].

There are just attempts to counteract and limit its progression through glycaemic control and lifestyle modifications, apprehending a great deal of scientific awareness to address novel treatment options to expedite peripheral nerve regeneration and provide better quality of life[4].

Experimental diabetic induction has been tried in prior scientific trials through different agents. Alloxan is one of the most prevalent diabetogenic agents as it is transported via glucose transporter 2 (GLUT2) into the pancreatic beta cells. It suppresses glucokinase activity and generates ROS with ultimate reduction in the number of β-cells, resulting in insulin deficiency[5].

Due to accumulative side effects of long-lasting consumption of conventional medicines, natural Plant-based medicines have emerged as an alternative regimen as they are affordable, widely accessible to rural populations, and have been associated with fewer aftereffects[6].

DOI: 10.21608/ejh.2025.377584.2256

Quercetin, one of the flavonoids has been proven to decrease blood glucose, to halt oxidative and inflammatory tissue damage[7].

Anticonvulsants are routinely prescribed by clinician in the treatment of a diabetic neuropathy[8].

Specifically, Topiramate possess its mechanism of action in the treatment of diabetic neuropathy through blockage of voltage dependent sodium and calcium channels, enhancement of GABA activity, together with an antioxidant property, hence can both decrease the neuropathic pain and control the pathogenesis of diabetic neuropathy[8].

MATERIAL AND METHODS

Material

Drugs and chemicals

Alloxan (Cat# 2244-11-3) was purchased as a powder from Sigma-Aldrich, St. Louis, USA. The required dose was weighed by a digital scale, freshly dissolved in normal saline and given as a single intraperitoneal injection.

Quercetin (Cat# Q4951-10G) was purchased as a powder from Sigma-Aldrich, St. Lòuis, USA. The required dose was weighed by a digital scale, dissolved in sesame oil and given by oral gavage.

Topiramate (Cat# 68462-0153-60) was purchased as tablets from Glenmark pharmaceutical company, USA. Each tablet contains 50 mg of topiramate. The required dose was calculated, dissolved distilled water, and given by oral gavage.

Animals

The current study was implemented using fifty adult male albino rats weighing 180-200 gram, aged 10–12 weeks at the animal house of Faculty of Veterinary medicine, Beni-Suef University. Each group was lodged in a separate hygienic cage; 5 rats / cage for the control group while 2 rats /cage for diabetic group due to high urine volume in a constant temperature (22–24 °C) and light-controlled room on an alternating 12:12 h light-dark phase. Rats were fed a standard commercial pellet diet with unrestricted food or water access to avoid dietary influence on diabetic induction and were acclimatized for one week before the launch of the experiment. The experiment has gotten the approbation from the Institutional Animal Care and Use Committee of Beni-Suef University (BSU-IACUC) (Approval No.024-054), Date 3/9/2024.

Experimental induction of diabetes

To institute a non-genetic rat model of type II DM, Alloxan injection was utilized as previously described[9]. Fastened rats received single intraperitoneal injection (IP) of freshly dissolved Alloxan (150 mg/kg body weight) into (2 ml/kg) distilled water. To avoid alloxan-induced hypoglycaemia, alloxan-treated rats were given access to 5% glucose solution overnight. 3days postinjection, blood samples were collected from the rats' tail veins, to assess the fasting blood glucose levels using an Accuò-Chek Active glucometer (Ròche Diagnostics, Monheim, Germanny). Rats with blood glucose levels exceeding 180 mg/dl for 2 successive measurements were selected to continue with the experiment as recommended by[10].

Animal grouping and treatment

1. Control group: Untreated control received basic chow only.
2. Experimental group (Alloxan-induced diabetic group: n=40): 4 weeks post diabetic induction, rats were allocated into 4 groups (each=10)[10] (Figure 1):

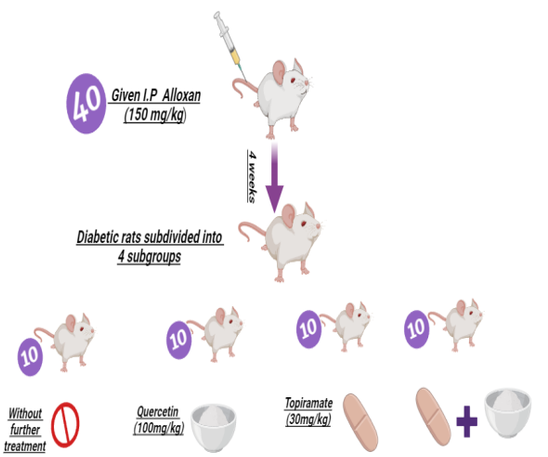

Fig. 1: Schematic representation of the experimental group subdivision

- Diabetic group (n=10): Rats kept diabetic[11].
- Quercetin treated diabetic group (n=10): Rats received Quercetin (100mg/Kg) by gastric gavage daily for 4 weeks[7].
- Topiramate treated diabetic group (n=10): Rats received Topiramate (30mg/kg) by gastric gavage daily for 4 weeks[12].
- Combined treatment diabetic group (n=10): Rats received Quercetin and Topiramate at the same dose and route as above.

Methods

At the end of the experiment, Blood samples were collected from retro-orbital veins then rats anesthetized with IP injection of 60mg/kg sodium pentobarbital (cat#p5178, Sigma-Aldrich, USA)[13]. Afterwards, rats were positioned on the op¬erating table in a prone position. Then, 3-cm of the skin was incised from the trochanter major muscle till the knee joint. The vastus lateralis and biceps femoris muscles were separated, and both sciatic nerves were rapidly dissected (Figure 2).

Fig. 2: A photograph showing the gross exposure of the sciatic nerve

Histological study

Left sciatic nerve specimen were fixed in 10% formalin saline, dehydrated in rising grades of ethanol and then embedded in paraffin, 4µm serial transverse sections were mounted on glass slides to be subjected to:

1. Hematoxylin & eosin (H&E) staining[14].

2. Immunohistochemical study[15].

Anti Caspase-3 antibody: Rabbit polyclonal anti-caspase-3 antibody (Diagnostic BioSystems, Cat# PR096, USA.) was afforded at dilution of (1:100)[11].

Anti S100 antibody: Rabbit polyclonal anti-S100 antibody (Proteintech, Cat#15146-1-AP, USA.). In neural regeneration experimental works[16] was provided at dilution of (1:500).

Each of the previously mentioned primary antibody was immunodetected through the labelled avidin-biotin-peroxidase complex (Histostain SP kit, Zymed Laboratories Inc, San Francisco, USA). Diaminobenzidine (DAB) was applied as a chromogen and Meyer's haematoxylin (Cat# 05-M06002) as a counterstain.

Ultrastructural study

The right sciatic nerve was sliced into multiple specimens, fixed in 2.5% phosphate buffered glutaraldehyde. Semithin sections about 1µm were sliced then stained with toluidine blue for about 45 seconds[17], which were subsequently examined by the light microscope with a (1000X) oil immersion lens. Ultrathin sections (about 80 nm) were obtained by the ultramicrotome then stained with heavy metals, first by uranyl acetate then by lead citrate. The ultrathin specimens were placed into TEM grid mesh to be analysed by JEOL electron microscope at 80 KV at Electron Microscope Unit of Faculty of agriculture, Cairo University.

Biochemical study

At the end of the experiment, after overnight fasting, blood samples were collected from the retro orbital veins using capillary tubes from all rats. Measurements were done at the Global research lab, Cairo, Egypt to assess the plasma levels of:

1. Plasma glucose level[18].
2. Malondialdehyde (MDA) as an oxidant marker[19].
3. Glutathione (GSH) as an antioxidant marker[20].
4. Tumour necrosis factor alpha (TNFα) as an inflammatory marker[21].

Morphometric study using image analyzer computer system

The data were obtained using "Leica Qwin 500 C" image analyzer computer system Ltd. (Cambridge, England) in histology department, faculty of medicine, Beni-Suef University. Images were captured live on to the screen from sections under light microscope with video camera. The image analyzer consisted of a colour video camera, Olympus microscope, coloured monitor, hard disc of IBM personal computer connected to the microscope and controlled by "Leica Qwin 500 C" software. The image analyzer was first calibrated to automatically convert the measurement units (pixels) produced by the image analyzer program into actual micrometer units. The obtained Data were expressed as a percentage of total tissue area.

The following parameters were measured:

1. The mean area percentage of the total nerve fibres in five randomly chosen non-overlapping fields from each toluidine blue stained section (X1000).
2. The mean ratio (G-ratio) between axonal diameter (µm) to the whole nerve fibre diameter (µm) in five randomly chosen non-overlapping fields from each toluidine blue stained section (X1000).
3. The mean area percentage of capase-3 immunoreactivity in immunohistochemically stained sections (X400).
4. The mean area percentage of S-100 immunoreactivity in immunohistochemically stained sections (X400).

Statistical analysis

Statistical analysis was carried out in SPSS (Version 15, Chicago, IL, USA). Results were expressed as mean values (±SD). Data was analyzed via One-way ANOVA followed by Tukey′s post-hoc tests to compare the means between the variant groups. A value of $P<0.05$ was considered significant[22].

RESULTS

Histological structural changes

Histological study using H&E (Figures 3-6)

Control group showed normal histo-architecture of the sciatic nerve with delicate connective tissues (endoneurium) outlining the closely related nerve fibres. Nerve fibre bundle was surrounded by CT sheath; perineurium and epineurium around the whole nerve (Figure 3a). Each myelinated nerve fibre was composed of central axon,

surrounded by nearly dissolved myelin sheath and flattened nuclei of Schwann cells. Fewer smaller unmyelinated nerve fibres were detected. The endoneurium connective tissue with its fibroblast was present in the spaces between the nerve fibres (Figure 3b).

Diabetic group demonstrated loss of the normal histo-architecture of sciatic nerve bundle. The perineurium appeared discontinuous and widely separated from the underlying shrunken degenerated nerve fibres. The nerve fibres appeared fragmented and lost in some areas with irregular or lost myelin sheath. Endoneurial oedema & mononuclear inflammatory cells were observed (Figure 4a). At a higher magnification, signs of axonal degeneration in form of axonal vacuolation was prominent; in addition to, vascular congestion with thickened basement membrane (Figure 4b). Other sections showed areas of myelin debris with the apparent decrease in the number of Schwann cell nuclei that existed as occasional dark pycnotic nuclei (Figure 4c).

Quercetin treated diabetic group demonstrated apparent improvement in the histo-architecture of the sciatic nerve compared to the diabetic subgroup. There was increase in the number of nerve fibres which became relatively close to each other and outlined by regular connective tissue perineurium. However, there were still congested blood vessels with some areas of missed fibres or endoneurial oedema. Other areas of degenerated nerve fibres were still observed (Figure 5a). At higher magnification, there was relative restoration of the normal histological features of the nerve fibres with occasional distorted, fragmented nerve fibres and others with degenerated central axons (Figure 5b).

Topiramate treated diabetic group demonstrated partial improvement in the histo-architectural appearance of most of the bundles of the sciatic nerve compared to the diabetic subgroup. However, other bundles still showed disorganized degenerated areas with parts of missed nerve fibres in between. The outer epineurium connective tissue was disturbed (Figure 5c). At a higher magnification, an incomplete improvement became more obvious, where some nerve fibres became relatively retained their normal histological features, while the others were still disorganized and degenerated (Figure 5d).

Combined Quercetin and Topiramate treated diabetic group (D-combined group) demonstrated nerve bundles with normal histo-architecture, when compared to the control group, formed of group of closely related nerve fibres outlined by outer dense epineurium and separated by perineurium with normal small blood vessels. Thin delicate connective tissue (endoneurium) in between the nerve fibres was seen (Figure 6a). At a higher magnification, nearby restoration of the normal histo-architecture became more obvious. Each myelinated nerve fibre was composed of central axon, surrounded by nearly dissolved myelin with other scattered unmyelinated nerve fibres. Fibers are outlined by outer intact connective tissue perineurium (Figure 6b).

Immunohistochemical study

A. Caspase-3 immuno-stained nerve sections (Figures 7, 8)

Control group showed negative immune-reactions while, the diabetic group showed extensive positive Caspase-3 immune-reactions in the axoplasm, epineurium, and perineurium. Diabetic groups treated either with Quercetin or Topiramate illustrated moderate positive immune-reactions in the axoplasm, vascular endothelium, and in the endoneurium of the nerve fibres surrounding blood vessel. On the other hand, the Diabetic combined treatment group revealed scanty positive immune reactions compared to diabetic group.

B. S100 immuno-stained nerve sections (Figures 9, 10)

The control group showed strong widespread S100 immune-reactions. Diabetic group showed weak immune reactions. While diabetic groups treated either with Quercetin or Topiramate showed increase in S100 immune-reactions. Contrary, combined treatment diabetic group revealed strong abundant positive immune reactions compared to the diabetic group.

Toluidine blue-stained semithin sections results (Figures 11, 12)

Control group showed a normal histological architecture of nerve bundles which appeared as closely related nerve fibres with variable sizes. Most fibres were myelinated with compact, dark myelin rings around the clear central axons. The same section showed few other unmyelinated fibres, forming ovoid cluster. Schmidt-Lanterman cleft was also detected (Figure 11a).

Diabetic group revealed apparent degenerative changes with occasional irregular lightly stained nuclei of Schwann cells. The myelin appeared thinner and irregular inform of either evagination or invagination and some with focal myelin splitting. Mast cell, macrophage, and mononuclear inflammatory cells were also seen detected (Figure 11b). Other sections showed most fibres with retracted and shrunken axons with increased peri axonal space, in addition to, congested blood vessel (Figure 11c).

With Quercetin administration to the diabetic group, some fibres appeared with intact myelin rings; however, there were still occasional fibres with either evagination, invagination, or focal myelin splitting. The fibres were outlined by intact outer perineurium and bounded together by inner endoneurium (Figure 12a).

Topiramate treated diabetic rats demonstrated part of nerve bundle with fibres widely separated from the overlying intact connective tissue; perineurium and epineurium. Still most fibres showed myelin sheaths irregularity and myelin splitting; in addition, to the presence of some retracted, shrunken central axons and irregular lightly stained nucleus of Schwann cell with mast cell in between (Figure 12b).

Combined treatment group revealed that almost all of the nerve fibres were with intact myelin rings and clear central axons. The fibres are closely related to each other, they are outlined by outer perineurium and bounded together by inner endoneurium. Mast cell and normal blood vessel lined by endothelium and surrounded with pericytes were detected with the presence of Schmidt-Lanterman cleft (Figure 12c).

Ultrastructural changes (Figures 13, 14)

Ultra structurally, control group illustrated multiple nerve fibres of different diameters. The most were myelinated nerve fibres ensheathed with thick compact regular electron dense myelin sheath, while the others form clusters of smaller unmyelinated nerve fibres (Figure 13a). Higher magnification illustrated Schwann cell wrapped around the myelinated axon, with its cytoplasm holding a normal nucleus with peripheral heterochromatin, mitochondria, rER, and Golgi apparatus and encircled by outer continuous basal lamina. In the same section, the axoplasm displayed electron dense particles representing; mitochondria, neurofilament and neurotubules (Figure 13b).

Diabetic group illustrated irregularity of the outline of multiple myelinated nerve fibres with extensive splitting of the myelin sheaths and compression of the central axons (Figure 13c). Other sections illustrated axonal degenerations, which appeared shrunken with cytoplasmic vacuolations representing swollen, degenerated mitochondria. Macrophage was detected with its eccentric nucleus with peripheral heterochromatin and foamy cytoplasm. In addition to, myelin sheath invagination and splitting (Figure 13d). Degenerated Schwann cell with irregular nucleus with more condensed heterochromatin and cytoplasmic vacuolations of large sizes; in addition to, area of myelin evagination (Figure 13e).

Quercetin treated diabetic group revealed that some myelinated fibres were regenerated with outer compact electron dense myeline sheath and central homogenous axons with apparently normal endoneurial blood vessel, mononuclear inflammatory cell, and mast cell. At the same section, other fibres still showed irregular outline inform of myelin splitting of invagination (Figure 14a). The regenerated central axons that displayed electron dense cytoskeleton of cytoplasmic content. The rims of the Schwann cells cytoplasm enclosing the fibres also showed tiny electron dense particles, representing glycogen rosette. The apparently normal endoneurial blood vessel was lined by endothelial cell resting on a basement membrane with outer flat pericyte. Two mast cells were detected with their electron dense cytoplasmic granules (Figure 14b).

Topiramate treated diabetic group illustrated multiple nerve fibres of different sizes. The myelinated nerve fibres owned nearly intact electron dense myelin sheathes central apparently normal axons, comparing to diabetic group, except for limited myelin lamellae splitting and minimal invaginations with the presence of clusters of smaller unmyelinated nerve fibres and a mast cell with its characteristic electron dense granules (Figure 14c). In other section (Figure 14d), there were still retracted, degenerated central axons that showed few dilated, disturbed mitochondria

The combined treatment group illustrated that most fibres are more or less normal with intact electron dense myelin sheaths and regenerated homogeneous central axons. Some fibres were wrapped by rims of Schwann cells (Figure 14e). Myelinated nerve fibre with a surrounding Schwann cell, displaying apparently normal nucleus with normal chromatin distribution, normal cytoplasmic density, and prominent basal lamina. The regenerated central axoplasm showed normal cytoplasmic organelles inform of mitochondria and smaller electron dense neurofilaments, when compared to diabetic group (Figure 14f).

Biochemical study

Blood glucose Levels: (Table 1, Histogram 1)

Blood glucose level value showed a significant increase (P<0.05) in diabetic group compared to the control group and the treated groups. While a significant decline (P<0.05) was noticed in the combined treatment group compared to diabetic Quercetin or Topiramate treated groups without a significant difference between the latter two groups.

Assessment of Malondialdehyde (MDA) and Reduced Glutathione levels (GSH): (Table 2, Histogram 2)

MDA and GSH values indicated a significant increase and decrease (P<0.05) respectively in diabetic group compared to the control group and all the treated groups. In addition, similar significance (P<0.05) was seen in diabetic-combined group compared to diabetic Quercetin or Topiramate treated groups without a significant difference between the latter two groups.

Assesment of tumour necrosis factor alpha (TNFα) Levels: (Table 3, Histogram 3)

TNFα value showed a significant increase (P<0.05) in diabetic-group compared to the control-group and the treated groups. In addition, similar significance was recorded in both diabetic groups treated either with Quercetin or Topiramate compared to the control and the combined treatment groups.

Morphometric and statistical results

Assessment of nerve fibres: (Table 4, Histogram 4)

The value of the area percent of the total nerve fibres was significantly declined (P<0.05) in diabetic group when compared to the control group and all the treatment groups.

Assessment of the ratio (G-ratio) between axonal diameter (µm) to the whole nerve fibre diameter (µm):(Table 4, Histogram 5)

The mean G ratio for diabetic group represented a significant decrease (P<0.05), compared to the control group and the treatment groups.

Assessment of S100 immunoreactivity: (Table 5, Histogram 6)

The mean area percentage of S100 immune reactions for diabetic group represented a significant decrease (P<0.05), compared to the control group and all the treatments groups.

Assessment of Caspase-3 immunoreactivity:(Table 5, Histogram 6)

Diabetic-group showed a significant upregulation of caspase-3 immune reactions (P<0.05), by comparison to the control group and

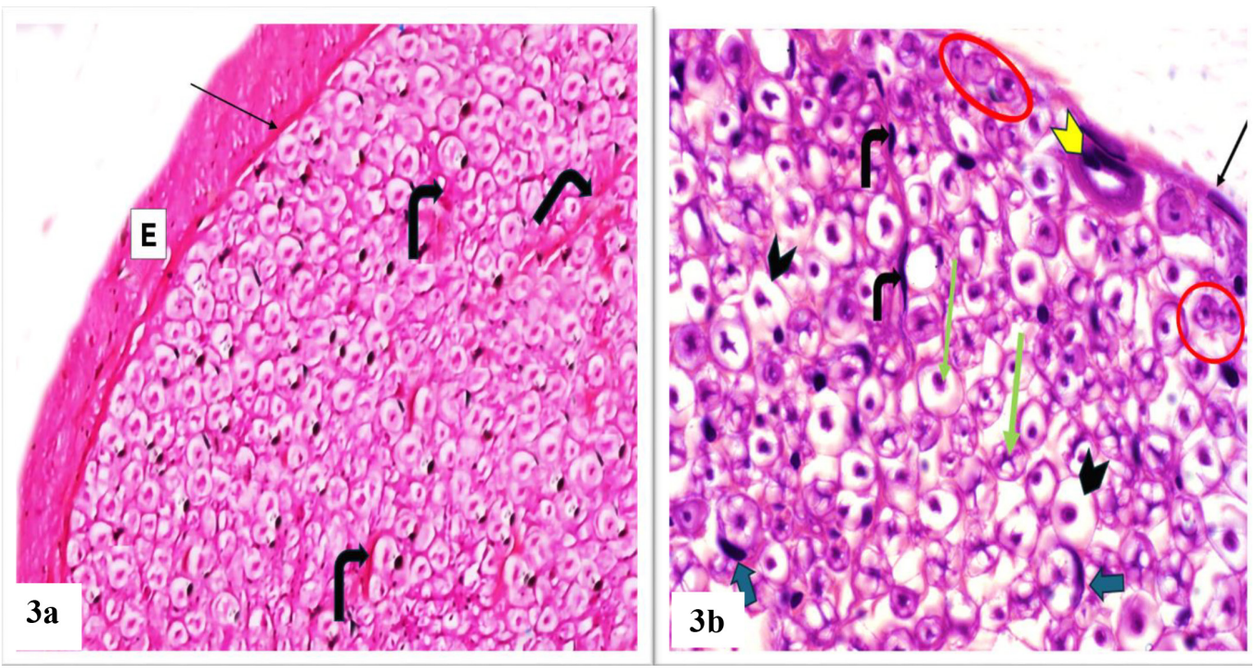

Fig. 3: Photomicrographs of sciatic nerve transverse sections from the control group stained with H&E. (3a) Showing part of nerve bundle with the normal histo-architecture, formed of group of closely related nerve fibers outlined by delicate connective tissues (endoneurium) (curved black arrows). The bundle is surrounded by CT sheath; perineurium (thin black arrow) then (epineurium) (E) (x400). (3b) Showing a part of nerve bundle, surrounded by the perineurium (thin black arrow). Each myelinated nerve fiber is composed of central axon (thin green arrows), surrounded by nearly dissolved myelin (black arrowheads) and flattened nuclei of Schwann cells (thick blue arrows) with fewer smaller unmyelinated nerve fiber (red circles) and normal blood vessel (yellow arrowhead). The endoneurium connective tissue with its fibroblast cell (black curved arrows) present in spaces between the nerve fibers (x1000).

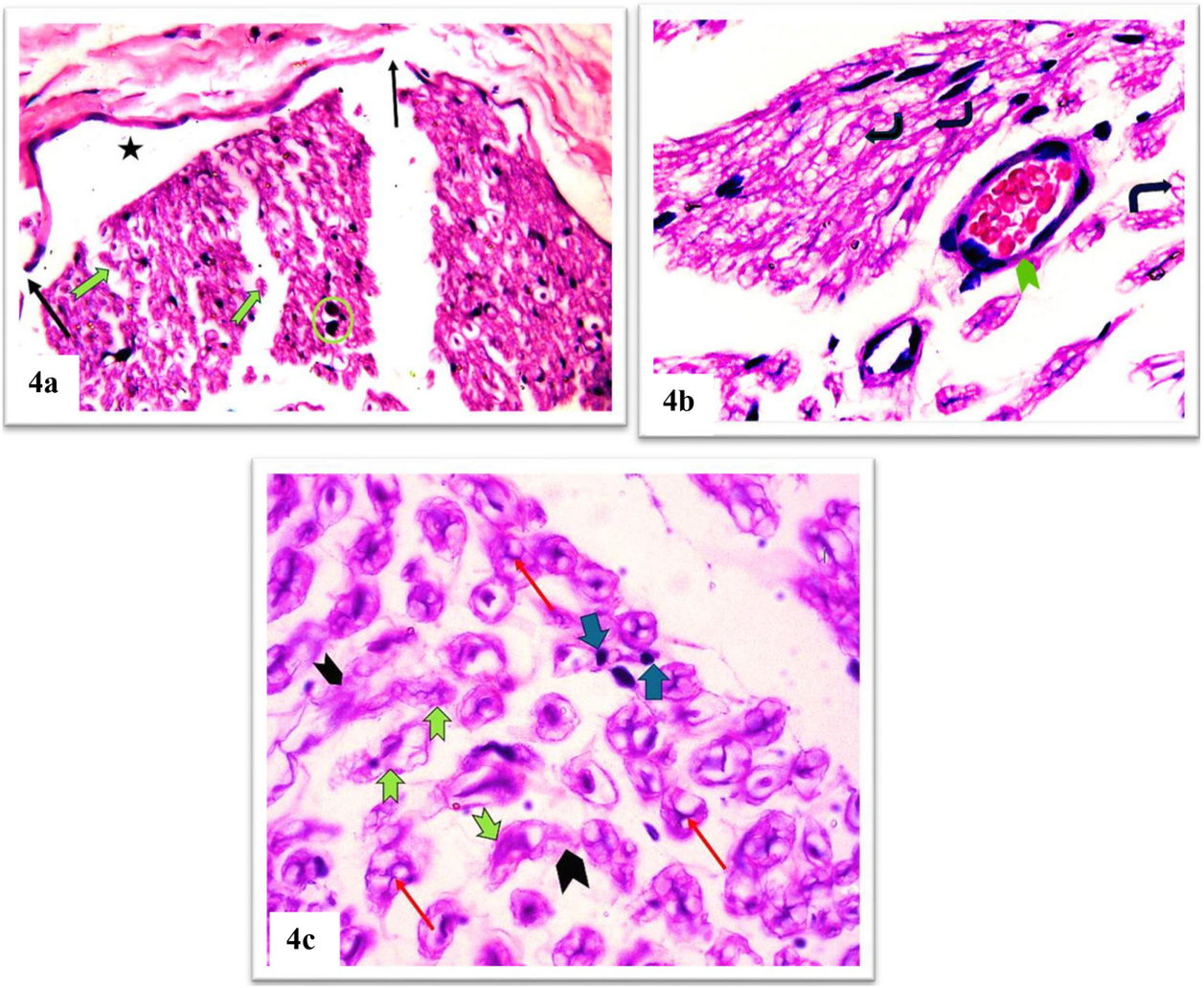

Fig. 4: Photomicrographs of sciatic nerve transverse sections from the diabetic group stained with H&E. (4a) Showing a loss of the normal histo-architecture of sciatic nerve bundles. The perineurium appeared discontinuous (thin black arrows) and widely discrete from the underlying shrunken degenerated nerve fibres, where nerve fibres appear fragmented, irregular, or lost myelin sheath (green notched arrows). Endoneurial oedema (black star) mononuclear inflammatory cells (green circle) are observed (x400). (4b) Showing part of nerve bundles with axonal vacuolations (black curved arrows) as a sign of axonal degeneration, and a congested blood vessel with thickened basement membrane (green arrowhead)(x1000). (4c) Revealing part of a nerve bundle demonstrating disorganized fragmented nerve fibres (green notched arrows) with retracted and shrunken axons (thin red arrows) and areas of myelin debris (black arrowheads). Notice the apparent decrease in the number of Schwann cell nuclei that exist as occasional dark pycnotic nuclei (thick blue arrows) (x1000).

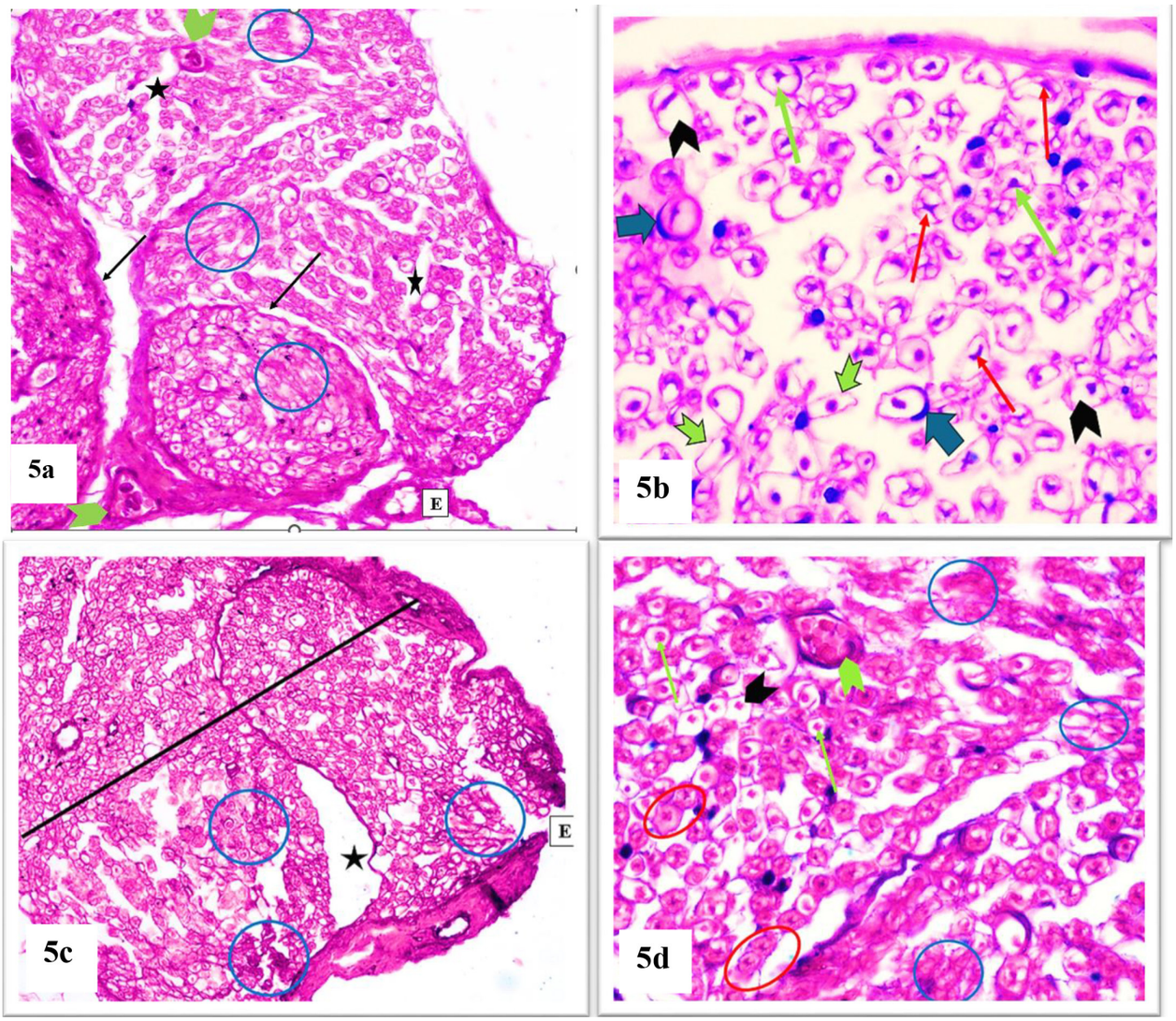

Fig. 5: Photomicrographs of H&E stained sciatic nerve from diabetic groups treated with Quercetin (5a, 5b) or with Topiramate (5c, 5d). (5a) Showing parts of nerve bundles demonstrating increase in the number of nerve fibres which become relatively close to each other and outlined by regular connective tissue perineurium (thin black arrows). However, there are still congested blood vessels (green arrow heads) with some areas of missed nerve fibres or endoneurial oedema (black stars) and other areas of degenerated nerve fibre (blue circles). Part of the outer thick connective tissue epineurium (E) is noticed (x400). (5b) Demonstrating a relative restoration of the normal histological features of the nerve fibres. Each myelinated nerve fibre is composed of central axon (thin green arrows), surrounded by nearly dissolved myelin (black arrow heads) and nuclei of Schwann cells (thick blue arrows), with occasional distorted, fragmented nerve fibres (green notched arrows) and others with retracted and shrunken axons (thin red arrows) (x1000). (5c) Showing partial improvement in the histo-architectural appearance of part of the nerve bundles (above the black line), while the others (below the black line) still showed disorganized degenerated areas (blue circles) with parts of missed nerve fibres or endoneurium oedema (black star) in between. The outer epineurium (E) was disturbed (x400). (5d)Some fibres become relatively close to each other and retain their normal histological features; central axon (thin green arrows) surrounded by nearly dissolved myelin (black arrowhead), while the others are still disorganized and degenerated (blue circles). Note the presence of some unmyelinated nerve fibres (red circles) and congested blood vessel (green arrowhead) (x1000).

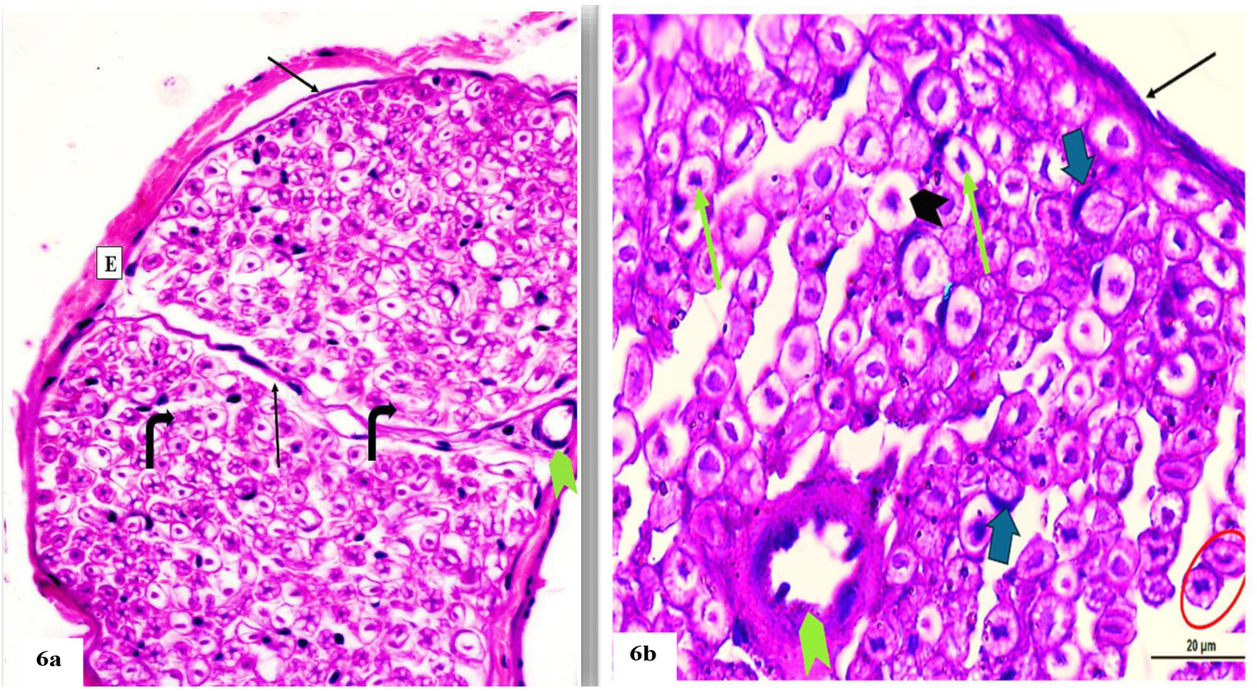

Fig. 6: Photomicrographs of H&E stained sciatic nerve from the combined treatment group. (6a) Showing two nerve bundles with normal histo-architecture, formed of group of closely related nerve fibres outlined by outer dense epineurium (E) and separated by perineurium (thin black arrows) with normal small blood vessels (green arrowhead). Thin delicate connective tissue endoneurium in between the nerve fibres (curved black arrows) (x400). (6b) Apart of a nerve bundle demonstrating nearby restoration of the normal histological features of the nerve fibres which appeared close to each other. Each myelinated nerve fibre is composed of central axon (thin green arrows), surrounded by nearly dissolved myelin (black arrowhead), other scattered unmyelinated nerve fibres (red circle) are detected. Outer intact connective tissue perineurium (thin black arrows). Notice the presence of Schwann cells (thick blue arrows) and the normal blood vessel (green arrowhead) (x1000).

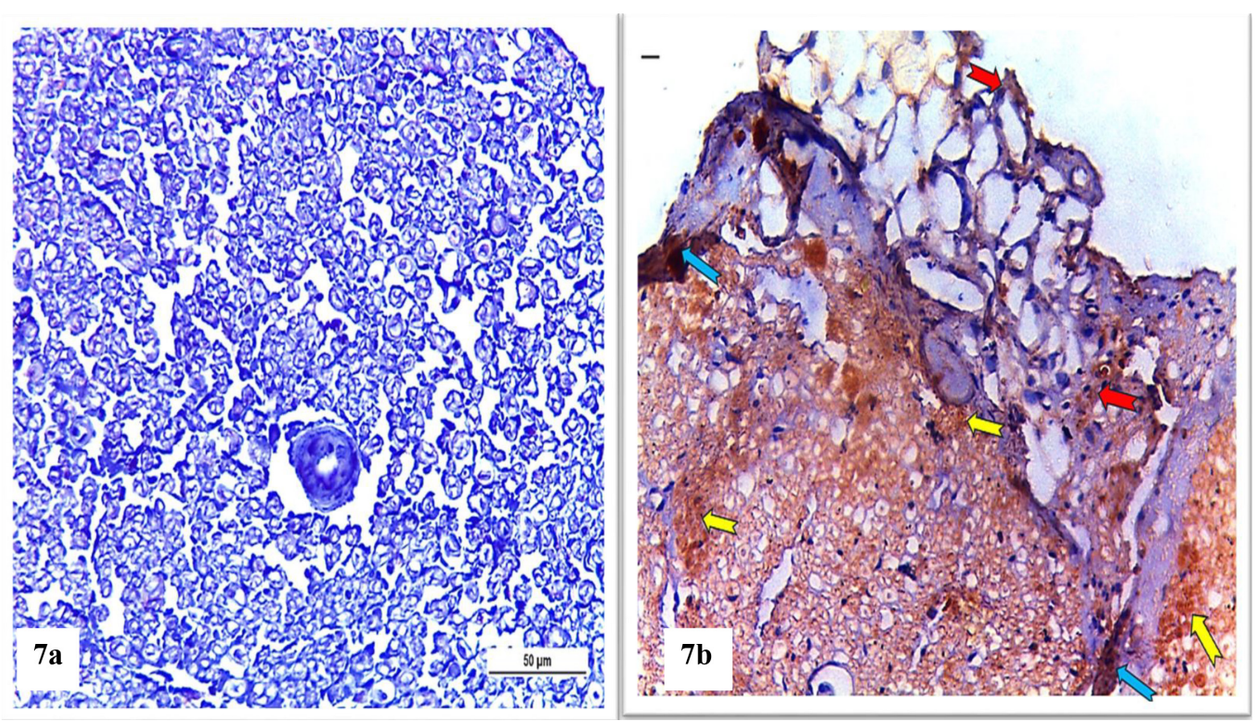

Fig. 7: Photomicrographs of sciatic nerve stained with anti-caspase-3 antibody. (7a) Control group demonstrates negative caspase-3 immune-reactions (x400). (7b) Diabetic group showing extensive positive Caspase-3 immune-reactions in the axoplasm of nerve fibres (yellow notched arrows), connective tissue epineurium (red notched arrow), and perineurium (blue notched arrows) in form of brown colourations (x400).

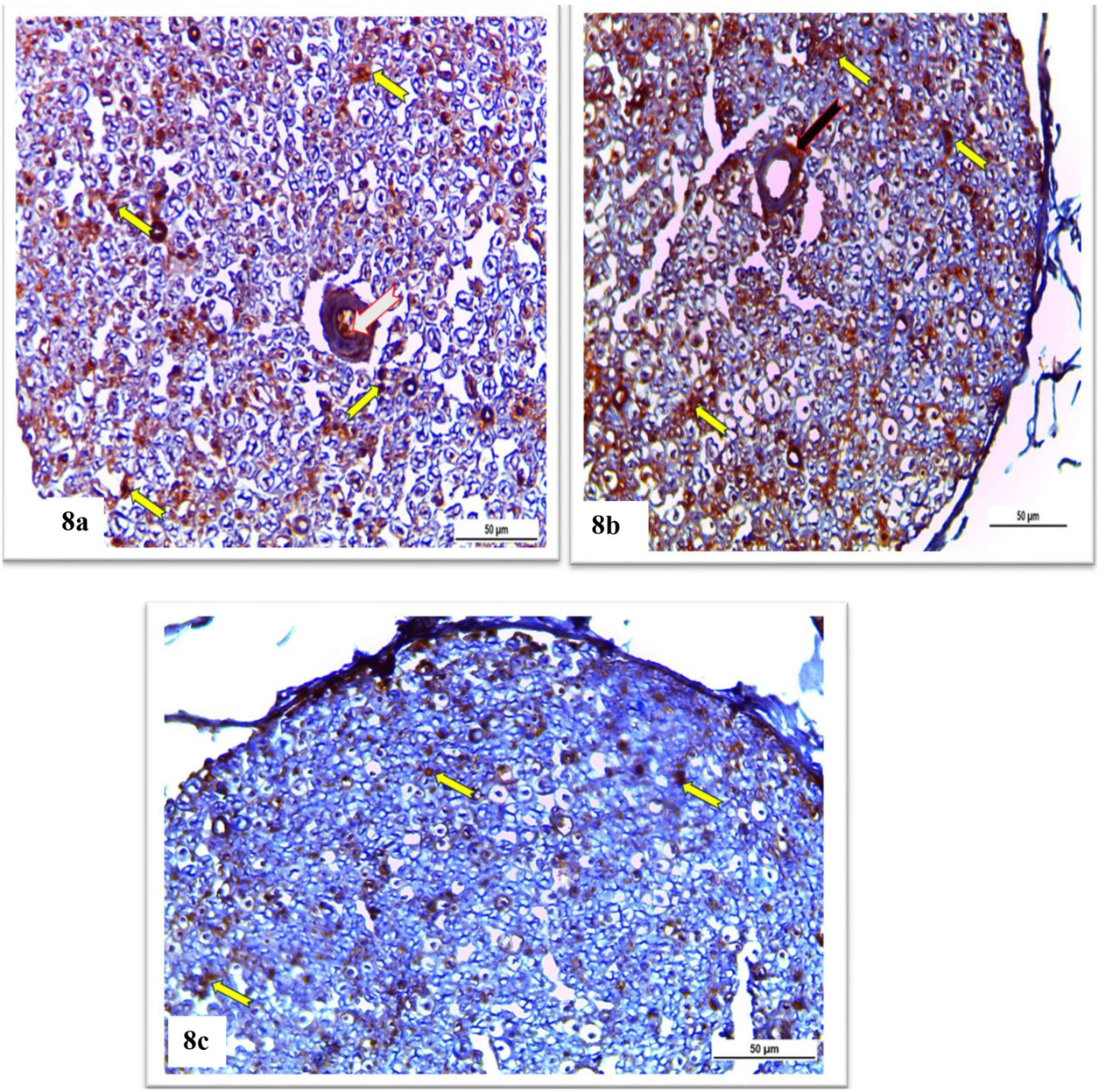

Fig. 8: Photomicrographs of sciatic nerve stained with anti-caspase-3 antibody (8a) Quercetin treated diabetic group showing moderate positive Caspase-3 immune-reactions in the axoplasm of nerve fibres (yellow notched arrows) and endothelium of the blood vessel (white notched arrow) in form of brown colourations (x400). (8b) Topiramate treated diabetic group showing moderate positive Caspase-3 immune-reactions in the axoplasm of nerve fibres (yellow notched arrows) and connective tissue endoneurium surrounding the blood vessel (black notched arrow) in form of brown colourations. (8c) Combined treatment group showing scanty positive Caspase-3 immune-reactions in the axoplasm of nerve fibres (yellow notched arrows) in form of brown colorations (x400).

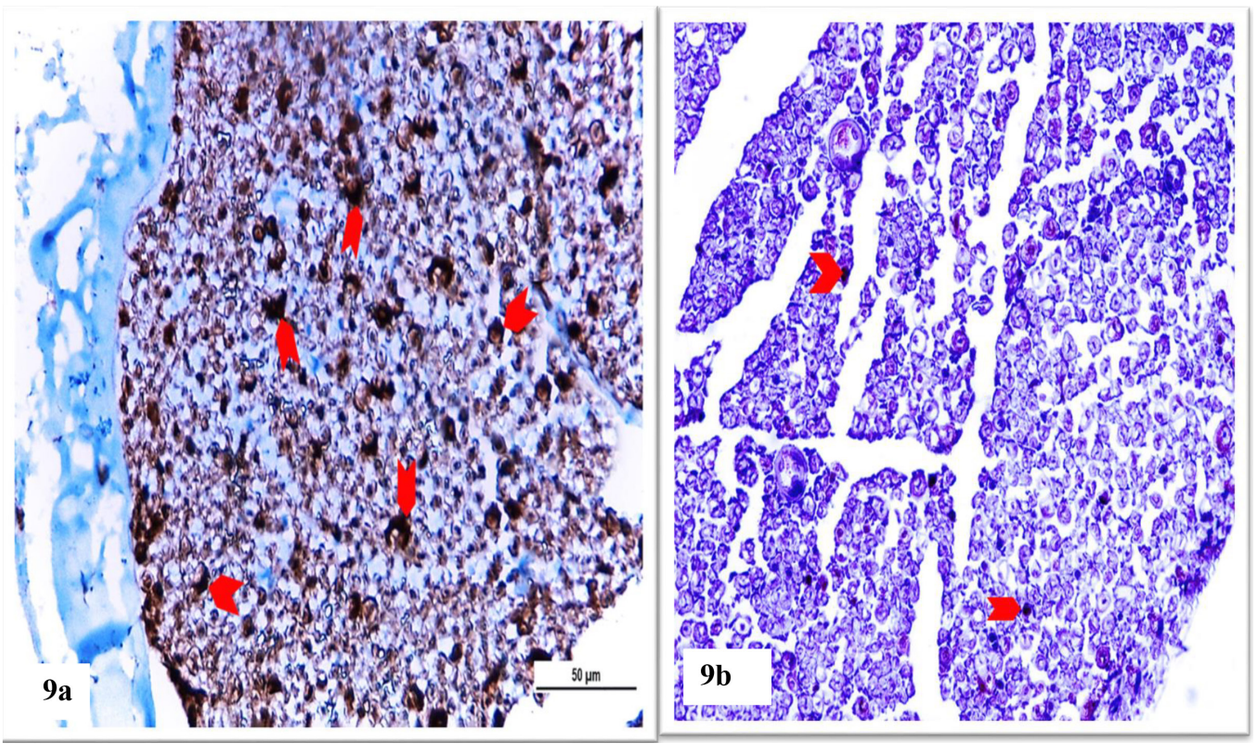

Fig. 9: Photomicrographs of sciatic nerve stained with anti-S100 antibody (9a): Control group showing strong widespread positive immune reactions in form of brownish granules (red arrow heads). (9b): Diabetic group showing few positive immune reactions in form of brownish granules (red arrow heads) against S-100 antibodies (x400).

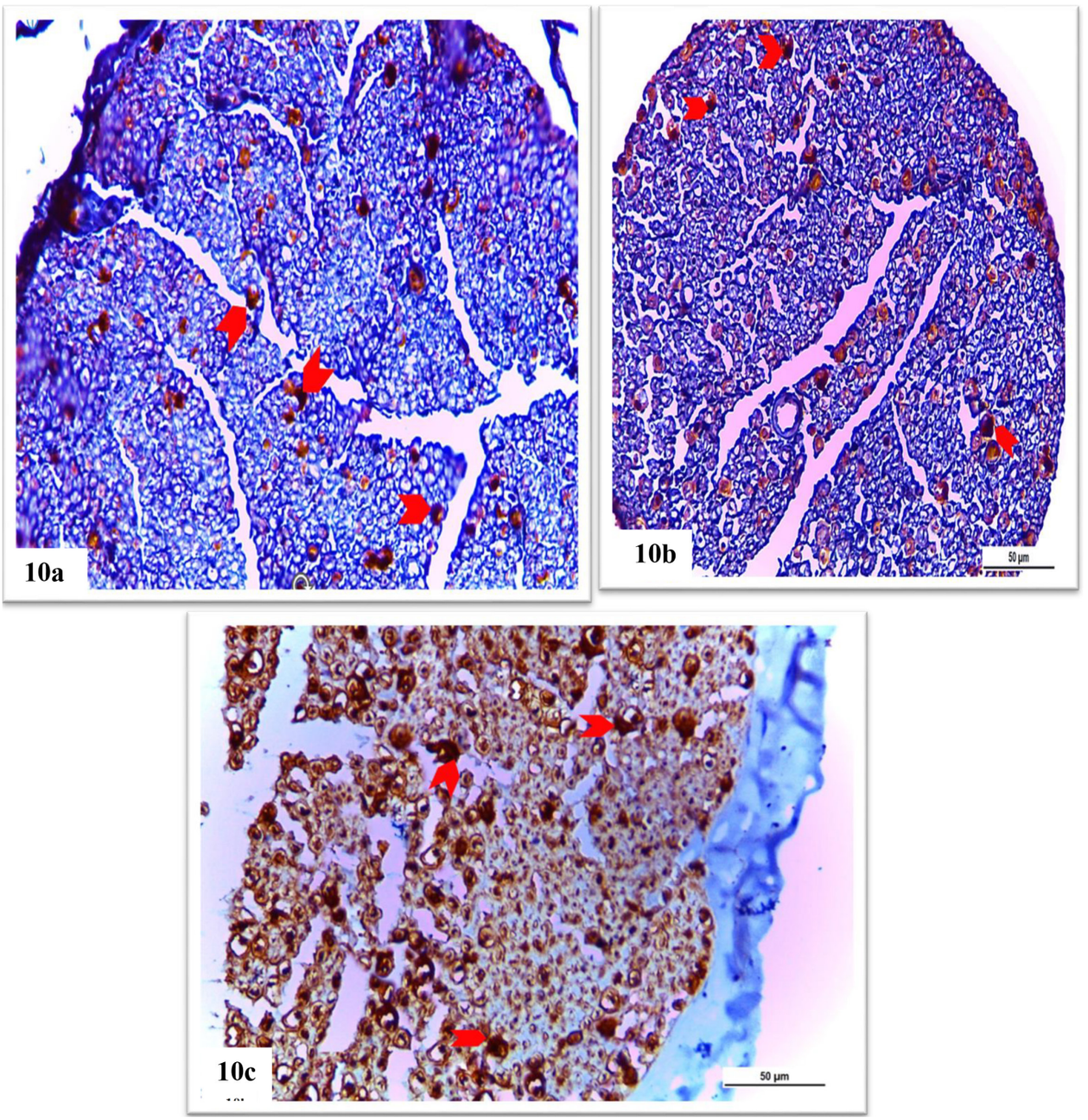

Fig. 10: Photomicrographs of sciatic nerve stained with anti-S100 antibody. Quercetin (10a) and Topiramate (10b) treated diabetic groups showing visible increase in the positive immune reactions in form of brownish granules (red arrow heads) against S-100 antibodies (x400). (10c) Combined treatment group showing strong abundant positive immune reactions in form of brownish granules (red arrow heads) against S-100 antibodies (x400).

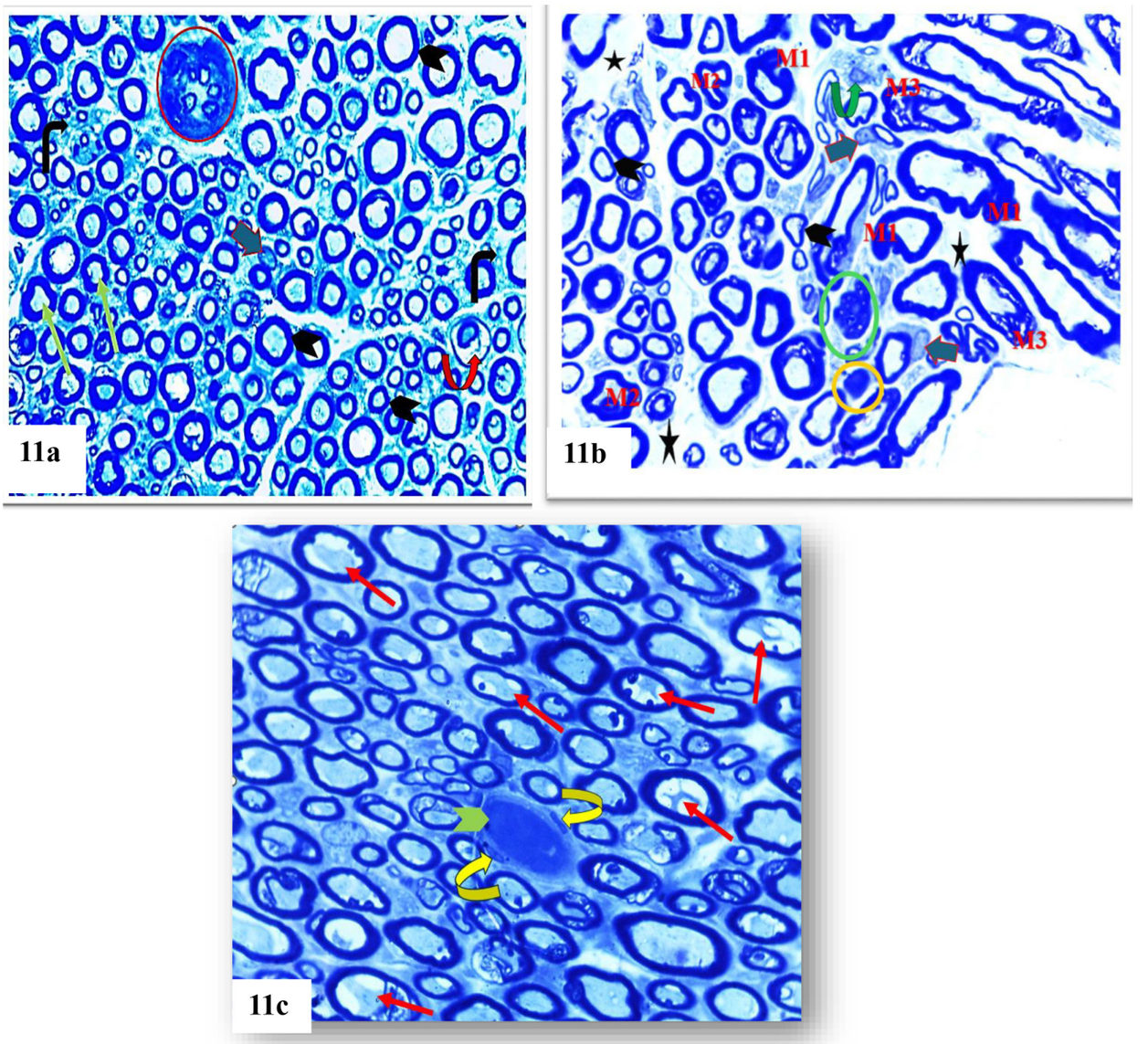

Fig. 11: Photomicrographs of sciatic nerve semithin sections. (11a) Control group demonstrating normal histological features with closely related nerve fibres with normal myelin sheath thickness, embedded in connective tissue endoneurium (black curved arrows). Most fibres were myelinated with dark, compact myelin rings (black arrowhead) around the clear central axons (thin green arrows) with few other unmyelinated fibres, forming ovoid cluster (red circle). Notice the presence of Schwann cells (thick blue arrow) and Schmidt-Lanterman cleft (red curved arrow). (11b) Diabetic group revealed apparent decrease in the numbers of nerve fibres that were separated from each other (black stars) with occasional irregular lightly stained nuclei of Schwann cells (thick blue arrows), myelin thinning (black arrow heads), and irregularity, inform of either evagination (M1) or invagination (M2) and some with focal myelin splitting (M3). Mast cell (green circle), macrophage with its foamy cytoplasm (curved green arrow), and mononuclear inflammatory cells (yellow circle) are also seen. (11c) Diabetic group demonstrating most fibres with shrunken and retracted axons with increased peri axonal space (thin red arrows); in addition to, congested blood vessel (green arrowhead) with the lining endothelial cells (curved yellow arrows) (x1000).

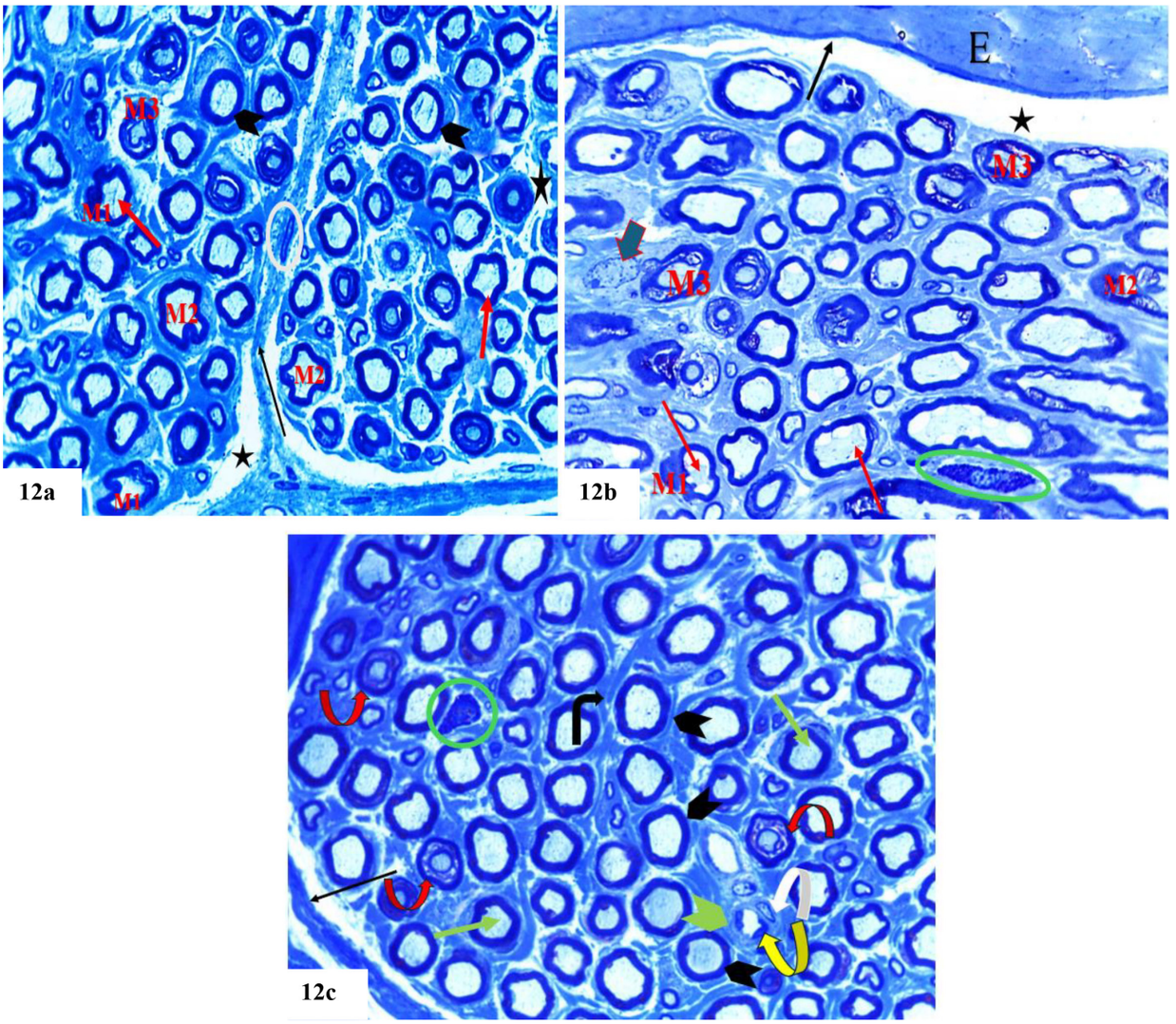

Fig. 12: Photomicrographs of sciatic nerve semithin sections. (12a) Quercetin treated diabetic group showing parts of two nerve bundles, separated by perineurium (thin black arrow) with fibroblast cell (white circle) and demonstrating limited areas of missed fibres or endoneurial oedema (black stars) with some fibres retained their outer intact myelin rings (black arrow heads); while others still show myelin sheaths irregularity inform of evagination (M1), invagination (M2), and myelin splitting (M3). There are still few retracted axons (red arrows). (12b) Topiramate treated diabetic group, the fibres are closely related to each other; however, they are widely separated from the overlying intact connective tissue; perineurium (thin black arrow) and epineurium (E) by an area of missed fibres or endoneurial oedema (black stars). Still most fibres show myelin sheaths irregularity inform of evagination (M1), invagination (M2), and myelin splitting (M3); in addition to the presence of some retracted, shrunken central axons (thin red arrows) with mast cell in between (green circle). Notice the presence of the lightly stained irregular Schwann cell nucleus (thick blue arrow). (12c) Combined treatment group, there is an apparent increase in nerve fibres, almost all of them with intact myelin rings (black arrow heads) and clear central axons (thin green arrows). The fibres are closely related to each other, they are outlined by outer perineurium (thin black arrow) and bounded together by inner endoneurium (curved black arrow). Mast cell (green circle) and normal blood vessel (green arrowhead) lined by endothelium (curved yellow arrow) and surrounded with pericytes (curved white arrow) are detected. Notice the presence of sign Schmidt-Lanterman cleft (red curved arrow) (x1000).

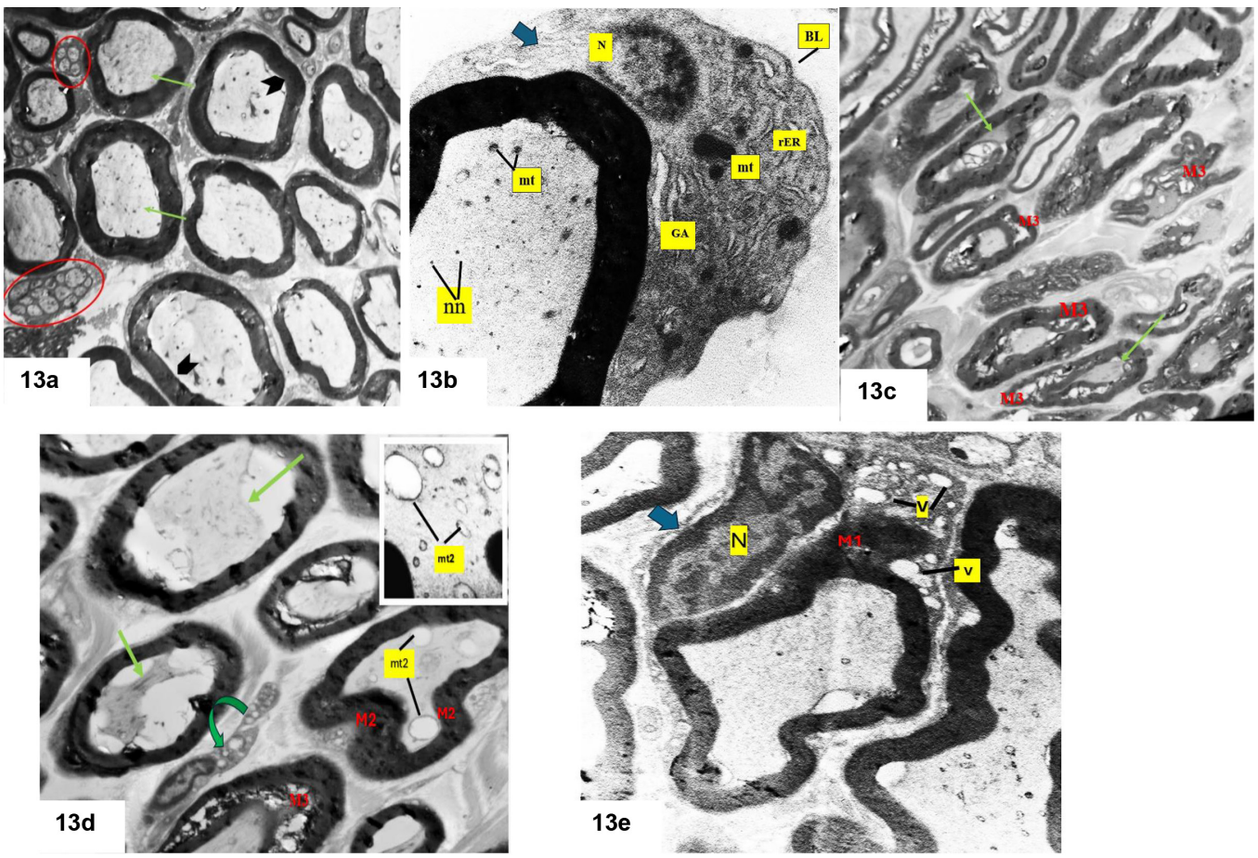

Fig. 13: Photomicrographs of sciatic nerve ultrathin sections from the control group (13a, b) and diabetic group (13C, D). (13a) illustrating multiple nerve fibres of different diameters. The most were myelinated nerve fibres ensheathed with thick compact regular electron dense myelin sheaths (black arrow) with central axons (thin green arrows), while the others form clusters of smaller unmyelinated nerve fibres (red circles) (X3000). (13b) Section in an axon showing the Schwann cell (blue arrow) wrapped around the myelinated axon, with its cytoplasm holding a normal nucleus (N), mitochondria (mt), and rough endoplasmic reticulum (rER), and Golgi apparatus with outer continuous basal lamina (BL). In the same section, the axoplasm displayed electron dense particles representing; mitochondria (mt), neurofilament and neurotubules (nn) (X10000). (13c) Illustrating irregularity in the outline of multiple myelinated nerve fibres with extensive splitting of the myelin sheaths (M3) and distortion of the central axons (thin green arrows) (X3000). (13d) Illustrating axonal degenerations, which appeared shrunken (thin green arrows). The central axon in the white boxed area is magnified to show the axonal cytoplasmic vacuolations representing swollen, degenerated mitochondria (mt2). Macrophage was detected with its eccentric nucleus with peripheral heterochromatin and foamy cytoplasm, denoting the phagosomes (green curved arrow). In addition to, myelin sheath invaginations (M2) and splitting (M3) (TEM X3000, inset X25000). (13e) Showing degenerated Schwann cell with irregular nucleus with more condensed heterochromatin (N) and cytoplasmic vacuolations of large sizes (V); in addition to, area of myelin evagination (M1) (X10000).

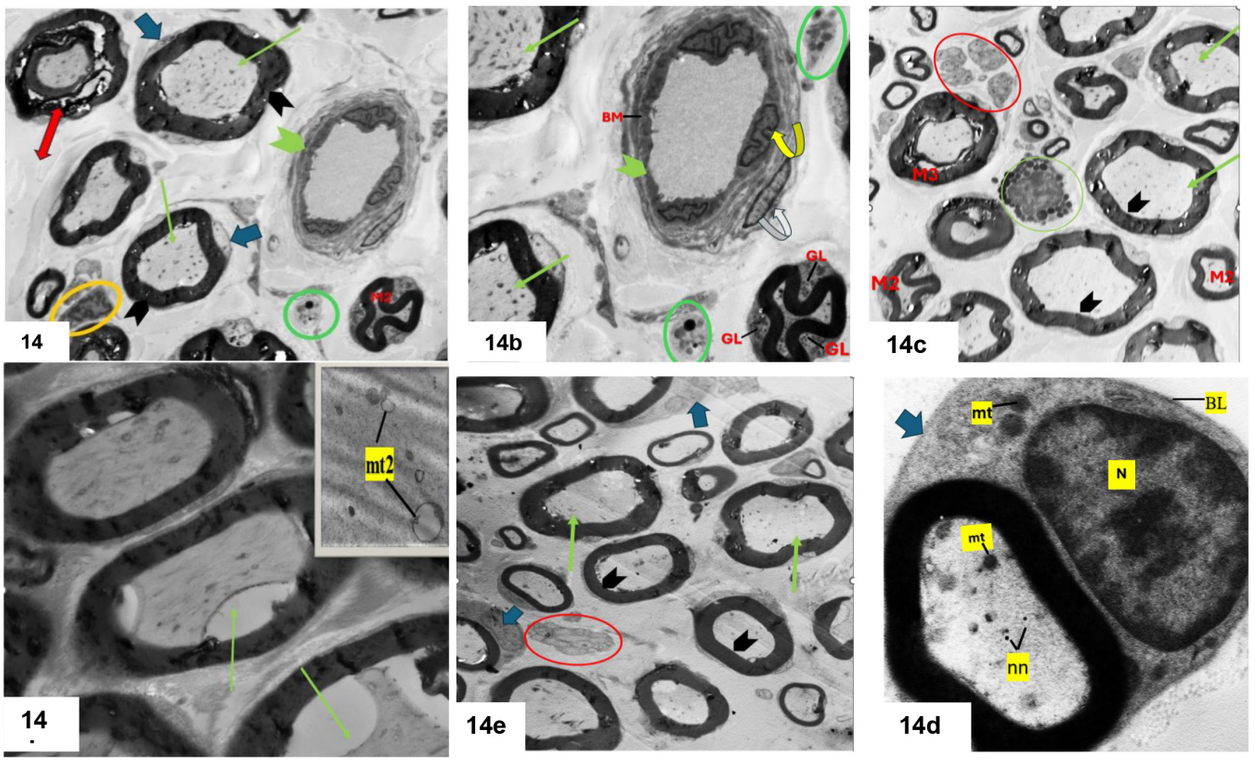

Fig. 14: Photomicrographs of sciatic nerve ultrathin sections from Quercetin (14a, b) and Topiramate (14c, d) and the combined (14e, f) treatment diabetic groups. (14a) Showing that some myelinated fibres are regenerated with outer compact electron dense myeline sheath (black arrow heads) and central homogenous axons (thin green arrows), surrounded by rims of Schwann cells (thick blue arrows) with apparently normal endoneurial blood vessel (green arrowhead), mononuclear inflammatory cell (yellow circle), and mast cell (green circle). At the same section, other fibres still showed irregular outline either inform of complete myelin lamellae splitting, as one fibre engulfing the other (double ended red arrow) or inform of myelin invagination (M2) (X3000). (14b) Illustrating regenerated central axons that displayed electron dense cytoskeleton of cytoplasmic content (thin green arrows). The rims of the Schwann cells cytoplasm enclosing the fibres also showed tiny electron dense particles, representing glycogen rosette (GL). The apparently normal endoneurial blood vessel (green arrowhead) was lined by endothelial cells (curved yellow arrow) resting on a basement membrane (BM) with outer flat pericyte (curved white arrow). Two mast cells (green circles) were detected with their electron dense cytoplasmic granules (X5000). (14c) Showing multiple nerve fibres of different sizes. The myelinated nerve fibres owned nearly intact electron dense myelin sheathes (black arrow heads) with central apparently normal axons (thin green arrows) except for limited myelin lamellae splitting (M3) and minimal invaginations (M2) with the presence of clusters of smaller unmyelinated nerve fibres (red circle) and a mast cell with its characteristic electron dense granules (green circle) (X3000). (14d) Showing retracted, degenerated central axons (thin green arrows) that showed few dilated, disturbed mitochondria (mt2), which are magnified in the white boxed area (X5000, inset X25000). (14e) Most fibres are more or less normal with intact electron dense myelin sheaths (black arrow heads) and regenerated homogeneous central axons (thin green arrows). Some fibres were wrapped by rims of Schwann cells (thick blue arrow). Notice the ovoid cluster of unmyelinated nerve fibres (red circle) (X3000). (14f) Revealing myelinated nerve fibre with a surrounding Schwann cell (thick blue arrow), displaying apparently normal nucleus with normal chromatin distribution (N), normal cytoplasmic mitochondria (mt), and prominent basal lamina (BL). The regenerated central axoplasm showed normal cytoplasmic organelles inform of mitochondria (mt) and smaller electron dense neurofilaments (nn) (X25000).

Table 1: Showing the mean ± standard deviation of serum glucose levels in the different groups.

Groups / Parameters	Glucose
C-group	84.317 ± 3.289
D-group	301.217 ± 3.782 $^{*\wedge@\#}$
D-Q group	142.167 ± 3.334$^{*+\#}$
D-T group	153.483 ± 1.799$^{*+\#}$
D-combined group	101.600 ± 2.344 $^{*+\wedge@}$
P- Value	0.000

Values expressed as Mean ± SD, * Significant VS C-group, + Significant VS D-group, ^ Significant VS D-Q group, @ Significant VS D-T group, #Significant VS D-combined group. Different superscripts (*, +, ^, @, #) indicate significant difference at *p-value* ≤ 0.05.

Table 2: Showing the mean ± standard deviation of serum MDA and GSH levels in the different groups.

Groups / Parameters	MDA	GSH
C-group	0.267 ± 0.048	5.797 ± 0.063
D-group	4.663 ± 0.235 $^{*\wedge@\#}$	3.733 ± 0.149$^{*\wedge@\#}$
D-Q group	1.913 ± 0.071 $^{*+\#}$	4.102 ± 0.266 $^{*+\#}$
D-T group	1.718 ± 0.043 $^{*+\#}$	4.188 ± 0.034 $^{*+\#}$
D-combined group	0.678 ± 0.035 $^{*+\wedge@}$	5.154 ± 0.161 $^{*+\wedge@}$
P- Value	0.000	0.000

Values expressed as Mean ± SD, * Significant VS C-group, + Significant VS D-group, ^ Significant VS D-Q group, @ Significant VS D-T group, # Significant VS D-combined group. Different superscripts (*, +, ^, @, #) indicate significant difference at *p-value* ≤ 0.05.

Table 3: Showing the mean ± standard deviation of TNFα in the different groups.

Groups / Parameters	TNFα
C-group	259.043 ± 10.611
D-group	519.675 ± 35.638$^{*\wedge@\#}$
D-Q group	363.085 ± 16.617$^{*+\#}$
D-T group	359.605 ± 2.900$^{*+\#}$
D-combined group	298.603 ± 6.427$^{*+\wedge@}$
P- Value	0.000

Values expressed as Mean ± SD, * Significant VS C-group, + Significant VS D-group, ^ Significant VS D-Q group, @ Significant VS D-T group, # Significant VS D-combined group. Different superscripts (*, +, ^, @, #) indicate significant difference at *p-value* ≤ 0.05.

Table 4: Presenting Mean ± SD of area % concerning the total nerve fibres and the G ratio in the studied groups as follows:

Groups / Parameters	G Ratio	Nerve Fiber Count
C-group	0.698 ± 0.059 $^{+\wedge\#}$	60.812 ± 2.232$^{+\wedge\#}$
D-group	0.293 ± 0.052$^{*\wedge\#\&}$	32.409 ± 2.577$^{*\wedge\#\&}$
D-Q group	0.518 ± 0.126 $^{*+\&}$	53.244 ± 1.7226$^{*+\&}$
D-T group	0.487 ± 0.144 $^{*+\&}$	52.521 ± 2.545$^{*+\&}$
D-combined group	0.706 ± 0.078 $^{*+\wedge\#}$	61.427 ± 3.162$^{*+\wedge\#}$
P- Value	0.000	0.000

Table 5: Presenting Mean ± SD of area % concerning S100 and Caspase-3 immunoreactivity in the studied groups:

Groups / Parameters	Caspase 3	S100
C-group	0.980 ± 0.215$^{+\wedge\#\&}$	31.094 ± 2.404$^{+\wedge\#\&}$
D-group	45.649 ± 3.936$^{*\wedge\#\&}$	2.7 ± 1.18$^{*\wedge\#\&}$
D-Q group	21.439 ± 3.023$^{*+\&}$	8.972 ± 1.059$^{*+\&}$
D-T group	20.531 ± 2.599$^{*+\&}$	8.779 ± 1.767$^{*+\&}$
D-combined group	7.689 ± 1.401$^{*+\wedge\#}$	23.418 ± 2.858$^{*+\wedge\#}$
P- Value	0.000	0.000

Values expressed as Mean ± SD (Area %), * Significant VS C-group, + Significant VS D-group, ^ Significant VS D-Q group, # Significant VS D-T group, while &Significant VS D-combined group. Different superscript (*, +, ^, # ,&) indicate significant difference at *p-value* ≤ 0.05.

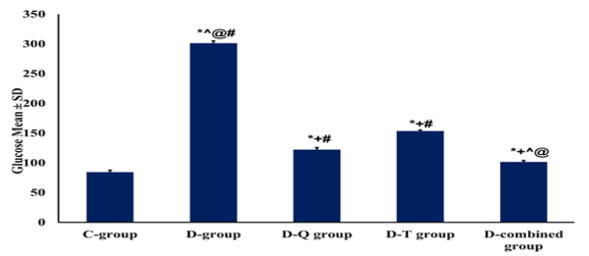

Histogram 1: Illustrating the mean values of serum Glucose levels in all the experimental groups.

Histogram 2: Illustrating the mean values of MDA and GSH serum levels in all the experimental groups.

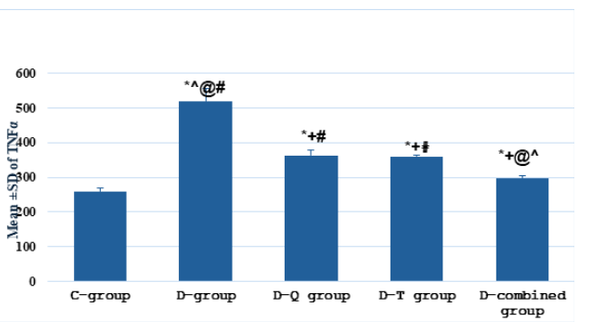

Histogram 3: Illustrating the mean values of TNFα serum levels in all the experimental groups.

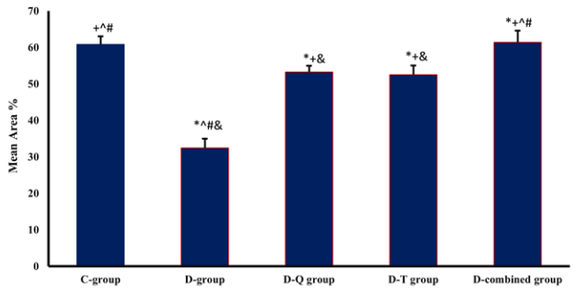

Histogram 4: Illustrating the mean values of the total nerve fibres count in all the experimental groups.

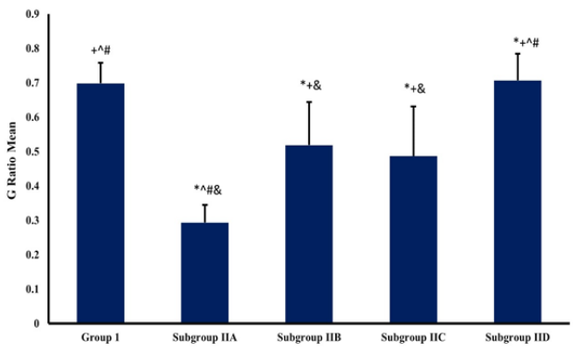

Histogram 5: Illustrating the mean values of G ratio in all the experimental groups.

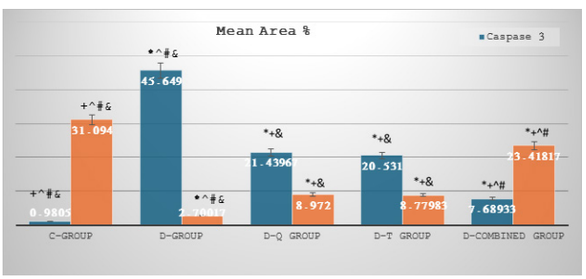

Histogram 6: Illustrating the mean values of S100 and Caspase 3 immunoreactivity in all the experimental groups.

DISCUSSION

The prevalence of Diabetes mellitus, a worldwide epidemic, has been rising steadily. The International Diabetes Federation (IDF) claims that the diabetic patients will reach up to 700 million by 2045[23]. Stemming from the chronic long-term hyperglycaemia, one-third of the diabetic patients suffer from diabetic neuropathy[4].

Sciatic nerve of albino rats was used in this study as a model of diabetic peripheral neuropathy due to the high similarity of both the anatomy and regenerative process between it and that of the human being. In addition, the sciatic nerve is the largest peripheral nerve so it can be easily examined and dissected[24].

The rationale design of this study aimed to shed light on the possible independent effects of both Quercetin and Topiramate, together with exploring their synergistic effects on the induced diabetic neuropathy.

The light microscopic examination of H&E-stained sciatic nerve sections from the diabetic group displayed overt degenerative alterations with loss of the normal sciatic nerve histo-architecture including the irregularity of the outer epineurium and disruption of the perineurium in between the nerve fascicles. As mentioned by Abedin *et al*., 2022[25], the composition of the extra-cellular connective tissue elements showed pronounced anomalies in the diabetic donors as the fibroblasts in these patients displayed a decreased ability to proliferate, migrate, and release their growth factors.

Meanwhile the current work illustrated that the nerve fibers in the diabetic group appeared severely disorganized as they were widely separated from each other and from the overlying perineurium by areas of nerve loss or endoneurial oedema. Recently Pereira *et al*., 2025[26] added that matrix metalloprotinease-9 is disintegrated from mast cells during the neural inflammation, providing a potential breaking down for the occludens and claudin molecules present in the tight junctions, causing a leaky blood-nerve barrier ending the oedema detected in the sciatic nerve sections of diabetic rats.

Additionally, Vaeggemose *et al*. (2020)[27] proposed that microvascular injury associated with diabetes is the most probable cause for focal fibre loss.

Other morphological alterations observed in diabetic group in the current work include either fragmented or degenerated nerve fibers with shrunken central axons and patches myelin debris. These outcomes align with prior study carried out by Sherikar *et al*., 2023[28], who also reported that chemically induced diabetes in animal models could cause Wallerian degeneration of peripheral nerve fibers, characterized by axonal degeneration and myelin breakdown. Similarly, the peripheral nerves are especially sensitive to oxidative stress due to their high metabolic activity, low antioxidant capacity, and non-replicative nature (Arisha, 2022)[10].

When Quercetin was administered to diabetic group in the current study, H&E-stained sections disclosed apparent improvements histo-architectural of the sciatic nerve to some extent. The nerve fibres were apparently increased in number and became relatively close to each other with a regular surrounding connective tissue. These histological outcomes justified by Muratori *et al*., 2022[29], who stated Quercetin has beneficial role in peripheral nerve protection and regeneration through its the anti-hyperglycaemic and antioxidant roles

Meanwhile, Mahmoud *et al*., 2023[30] stated that Quercetin supplementation is associated with elevation of

serum nerve growth factor (NGF), a crucial neurotropin concerned with neuronal development and regeneration with subsequent apparent increase in the number of nerve fibres. Although the histological alterations were lessened in diabetic rats treated with quercetin alone, the structural architecture of Sciatic nerve still appeared unlike the control ones.

H&E-stained Sciatic nerve sections of the Topiramate treated diabetic group displayed regression of the degenerative changes in the Sciatic nerves of the diabetic rat, which was still incomplete, where part of the nerve fibres retained their normal histological features while the others were still degenerated and widely separated from each other. The neuro-regenerative capability of Topiramate outstand not only from its antioxidant and anti-inflammatory capacity but also from being glutamate receptors antagonist[31].

The optimal histo-architecture improvements were clearly shown in the H&E stained-sections from the combined treatment diabetic group in form of closely packed nerve fibres outlined by regular, intact stromal coverings

Toluidine-blue semithin sections from the diabetic group revealed apparent decrease in the numbers of nerve fibres that were separated from each other with myelin irregularity, inform of either evagination or invagination and some with focal myelin splitting.

Meanwhile, the previously mentioned morphological alternations go hand in hand with Gopalan, 2024[23]. To our knowledge the level of nerve growth factor (NGF) that is involved in neurite growth is declined in cases of diabetes with subsequent decline in nerve fibres quality and quantity due to neurons apoptosis with consequent decrease in nerve fibres count[32].

The perceived myelin irregularity in the present study was also previously recorded by Hsueh *et al*., 2025[33], who found that the myelin sheath of the sciatic nerves in the diabetic models characterized by its irregularity and bulging either toward the axonal or the stromal side.

Another crucial finding in this work was the invasion of Mast cells, macrophages, and mononuclear inflammatory cells. It is known widely that plentiful neuropathological disorders are influenced extensively by the crosstalk between the immune and nervous systems[34].

Further approvement for the histological degenerative observations detected in this work in the semi-thin sections of the diabetic group was performed via statistical morphometric analysis which showed that mean area % of the total number of nerve fibres and G ratio (axonal diameter/ whole fibre diameter) in the diabetic group was significantly compromised (*P value*< 0.05) in relation to that of the control group and all the treated groups.

Considering Quercetin treatment, Toludine blue stained semi-thin sections of Quercetin treated diabetic group exhibited a histological improvement; however, it didn`t fully achieve the normative features. The nerve fibres coherence seemed to be integral except for limited areas of missed fibres. Regarding regularity of myelin sheath, some fibres retained their outer dark-blue myelin sheath, while others still appeared with invagination, evagination, or splitting. Corroborating with impact of Quercetin in retaining the myelin sheath integrity in current study, Song *et al*., 2024[35] elucidated that Quercetin upgrades the expression of myelin regeneration associated proteins as myelin basic protein and myelin protein zero.

The degenerative histological features revealed partial tendency toward the regeneration in the semi-thin sections of Topiramate treated diabetic group with apparent increase of nerve fibres, inconsistent with Sherikar at al., 2023[8] finding. Correspondingly, Topiramate can also inhibit the activity of voltage-gated calcium channel, decreasing ca+ influx that promotes neuronal apoptosis, hence giving more chance for the process of peripheral nerve regeneration[36].

Concerning the histological examination of the semi-thin sections of combined treatment diabetic group, we morphologically identified an apparent increase in the number of nerve fibres. Almost all the myelinated fibres appeared with regular-thick myelin sheath with mast cell noticed within the endoneurium beside an apparently normal blood vessel. Previously, Hsueh *et al*., 2025[33] emphasized that mast cells have a pivotal role during the regenerative process through their mediators that incite the differentiation of the mesenchymal cells to Schwann cells, a glial cell crucial for nerve sprouting; as well as other angiogenic mediators, affording a suitable circumstance for peripheral nerve regeneration.

As the quantification of the total number of nerve fibres is an important measurement to assess the neural regeneration, we validate the regeneration in the semi-thin sections of combined treatment diabetic group by morphometric analysis of the total numbers of nerve fibres along with the G-ratio to find that there was a significant elevation (*P value*< 0.05) in relation to the diabetic group and all other treated groups.

In the present work, Sciatic nerve sections of diabetic group evaluation for Caspase-3, they revealed a marked elevation of Caspase-3 immune response, aligned with previous studied which stated that there is evidential crosstalk between hyperglycaemia induced oxidative stress and cellular apoptosis[31].

Conversely, both Quercetin and Topiramate treated diabetic groups exhibited down regulation of Caspase-3 immune-reactivity to some extent, while the marked decline in Caspase-3 immune-reactivity recorded in the combined treatment diabetic group. Significant elevation (*P*<0,05) in the mean area % of Caspase-3 immun-reactivity in diabetic group in relation to control group and all the treated groups, while combined treatment diabetic group revealed significant decline (*P*<0,05) as compared to Quercetin and Topiramate treated diabetic group.

S-100 protein is related to a family of low molecular weight acidic proteins found in the Schwann cells to play a role in the regenerative process of the nervous system[37].

In the current work, diabetic group revealed marked downgrading for anti-s100 immune expression. Meanwhile, concomitant administration of Quercetin and Topiramate in combined treatment diabetic group succussed in upgrading the expression of S-100 obviously in correlation with diabetic group and the treated groups with Quercetin or Topiramate.

These interpretations were in harmony with previous work conducted by Amin *et al*., 2024[38], who discovered that animals treated with topiramate had increased level of S-100 and with Abdel Ellatif *et al*., 2023[11], who stated that flavonoid administration, including Quercetin, was found to increase the S-100 expression in sciatic nerve sections.

Through our morphometric analysis, the mean area % of S-100 expression is statistically low (P<0,05) in diabetic group compared to control group and all the treated groups, while combined treatment diabetic group elucidated the highest significant rise (P<0,05) in the mean area %, pointing to that the most favourable degree of regeneration occurred in the sections of combined therapy group.

The major ultrastructural degenerative alternations were observed in the ultrathin sections of the diabetic rats in diabetic group, where the majority of the myelinated nerve fibres showed extensive splitting of the myelin sheath and distorted, degenerated central axons.

During the pathogenesis of DPN, certain signalling pathways are activated within the Schwann cell, as high polyalcohol pathway flux by the effect of the oxidative stress, mitochondrial dysfunction, dyslipidaemia, and inflammation associated with the hyperglycaemic state. Activation of these pathways lead to sustained elevation in the levels of glycolysis, ROS formation, and deoxyribonucleic acid (DNA) methylation. These alterations ultimately leading to myelin splitting and destruction[39]. According to Ibrahim *et al*., 2024[12], DPN is associated with significant decline in neurofilament heavy chain protein (NEFH), a crucial cytoskeleton protein involved in maintenance of the axonal integrity, ending with axonal disintegration and degeneration.

Other ultrathin sections of diabetic group showed cytoplasmic vacuolation within the axoplasm and the cytoplasm of Schwann cell. Cheng *et al*., 2024[40] found corroborating results that can be attributed to mitochondrial damage inform of swollen mitochondria with destructed cristae.

In the present study the nucleus of the SCs in diabetic group appeared with irregular outline with more condensed heterochromatin reaffirming Schwann cell dysfunction and apoptosis

Subsequently to 4 weeks treatment with Quercetin, ultrastructural examination of the Sciatic nerves from Quercetin treated diabetic group exhibited lesser degree of degenerative configuration, Parallel to these findings, Fideles *et al*., 2023[41] claimed that Quercetin administration evaluate the expression of certain proteins that participate in myelin sheath conservation and integrity, including myelin-associated protein (Mag) and peripheral myelin protein 22 (pmp22), as well as the expression of growth associated protein 43 (Gap 43) and neurofilament 200 (NF200) that are involved in axonal growth and regeneration.

Ultrastructural examination of Topiramate treated diabetic group in this work revealed regression in the degenerative features as most myelinated nerve fibres owned nearly intact electron dense myelin sheathes with central apparently normal axons. In agreement, Ibrahim *et al*., 2024[12] stated that topiramate administration upgrade the expression of Gap 43, a protein needed for axonal growth and the expression of Neuron-Glial Antigen-2 (NG-2), a precursor cell helps in the process of re-myelinisation.

In current work, we found that the concomitant administration of Quercetin and Topiramate for 4 weeks in combined treatment diabetic group yielded better ultrastructural recovery. Schwann cell displayed apparently normal nucleus with normal chromatin distribution with normal cytoplasmic mitochondria and prominent basal lamina.

As the hyperglycaemia is the principal feature of DM, serum blood glucose was assayed in all the studied groups at the end of the experiment. The obtained data revealed rats in diabetic group depicted a highly elevated serum glucose level (*P value*< 0,05) when compared with the other subgroups.

Although the pathogenesis of DPN is multifaceted, creation of oxidative stress environment by the state of chronic hyperglycaemia is considered the major player by which diabetes can induce peripheral neuropathy[42]. For this reason, effectual antioxidant therapies as Quercetin and Topiramate have become essential in the regimens in the management of DPN[43]. To gain insight into this hypothesis, we evaluated the levels of both Malondialdehyde (MDA), a biomarker indicating the level of oxidative stress and Glutathione (GSH) a pivotal endogenous antioxidant enzyme in all the experimental group.

Our biochemical assessment revealed that the serum level of MDA and GSH in the diabetic group showed significant increase and decrease (*P value*< 0,05) respectively. However, combined treatment diabetic group significantly (*P value*< 0,05) decreased the serum level of MDA and elevated the level of GSH correlated to those of other groups

To investigate the role of inflammation in the DPN, we measure the level of TNFα in current studied group and we found that there was a significant rise (*P value*< 0,05) in the diabetic group, while combined treatment diabetic group significantly lessen (*P value*< 0,05) the

serum level of TNFα in relation to the other group ; however, still significantly higher that control group. The forementioned data was in line with Fideles *et al*., 2023[41], who pronounced that Quercetin reduces the liberation of the inflammatory cytokines and with Mohos *et al*., 2024[44] who described that Topiramate suppresses the activation of microglial cells in PNs and thus the release of TNF α.

Making all of our histological, biochemical, and morphometric results in mind we can hypothesize that the concomitant administration of Quercetin and Topiramate, they can act synergistically in escalating the regenerative capacity of the peripheral nerve, suffering from the diabetic neuropathy and obtaining a satisfactory recovery level.

CONCLUSION

The present work clearly demonstrates that:

- Alloxan administration could be able to achieve a state of hyperglycaemia in animal models.
- Chronic hyperglycaemia is one of the leading causes of peripheral neuropathy.
- Concomitant Quercetin and Topiramate therapy with exerted pronounced amelioration of the previously mentioned histological, biochemical, and morphometric alternations compared to individual therapy of either Quercetin or Topiramate.

RECOMMENDATIONS

- The probable risks of long-term administration of Topiramate and Quercetin still need further in-depth evaluation.
- The need for study of the therapeutic impact of combined Quercetin and Topiramate in clinical studies on volunteer subjects presenting with DPN, serving the medical field and clarify the exact mechanism by which this combined therapeutic regimen provides neurological regeneration.

CONFLICT OF INTERESTS

There are no conflicts of interest.

REFERENCES

1. Nemoto, W., Yamagata, R., Nakagawasai, O., Hoshi, T., Kobayashi, R., Watanabe, M., & Tan-No, K. (2025). Spinal ADAM17 contributes to the pathogenesis of painful diabetic neuropathy in leptin receptor-deficient mice. Biochemical Pharmacology, 116780. DOI: 10.1016/j.bcp.2025.116780
2. Jadhao, P., Swain, J., Das, S., Mangaraj, S., & Sravya, S. L. (2025). Prevalence and predictors of diabetic peripheral neuropathy in newly diagnosed type 2 diabetes mellitus patients. Current Diabetes Reviews, 21(3), e120224226871. DOI:10.2174/0115733998282818240125110248.
3. Hashim, M., Akhtar, J., Khan, M. I., Ahmad, M., Islam, A., & Ahmad, A. (2024). Diabetic Neuropathy: An Overview of Molecular Pathways and Protective Mechanisms of Phytobioactives. Endocrine, Metabolic & Immune Disorders-Drug Targets (Formerly Current Drug Targets-Immune, Endocrine & Metabolic Disorders), 24(7), 758-776. DOI: 10.2174/0118715303266444231008143430.
4. Barbosa-Ferreira, B. D. S., Silva, F. E. R. D., Gomes-Vasconcelos, Y. D. A., Joca, H. C., Coelho-de-Souza, A. N., Ferreira-da-Silva, F. W., & Silva-Alves, K. S. D. (2024). Anethole Prevents the Alterations Produced by Diabetes Mellitus in the Sciatic Nerve of Rats. International Journal of Molecular Sciences, 25(15), 8133. DOI: 10.3390/ijms25158133.
5. Moustafa, M. H., Turkey, M. S., Mohamedin, N. S., Darwish, A. A., Elshal, A. A., Yehia, M. A., & Mohamed, E. I. (2024). Eggshell membrane and green seaweed (Ulva lactuca) micronized powders for in *vivo* diabetic wound healing in albino rats: a comparative study. Journal of Pharmaceutical Health Care and Sciences, 10(1), 43. DOI:10.1186/s40780-024-00345.
6. Ahmed, R., Pavithra Kumari, H. G., Charan, V., Kousalya, P., & Shukla, C. P. (2025). The Role of Medicinal Plants in Managing Diabetes Mellitus: A Systematic Review. Cuestiones de Fisioterapia, 54(3), 513-534.
7. Türedi, S., Çelik, H., Dağlı, Ş. N., Taşkın, S., Şeker, U., & Deniz, M. (2024). An Examination of the Effects of Propolis and Quercetin in a Rat Model of Streptozotocin-Induced Diabetic Peripheral Neuropathy. Current Issues in Molecular Biology, 46(3), 1955-1974. DOI: 10.3390/cimb46030128
8. Sherikar, A. K., Upaganlawar, A. B., & Upasani, C. D. (2023). Effect of Topiramate on Mitochondrial Biogenesis and Neuroinflammation in Chronic Constriction Injury and Streptozotocin-induced Peripheral Neuropathy. Indian Journal of Pharmaceutical Education and Research , 57(3s), s626-s638. DOI: 10.5530/ijper.57.3s.71
9. Aslam, B., Hussain, A., Sindhu, Z. U. D., Nigar, S., Jan, I. U., Alrefaei, A. F., & Khan, R. U. (2023). Polyphenols-rich polyherbal mixture attenuates hepatorenal impairment, dyslipidaemia, oxidative stress and inflammation in alloxan-induced diabetic rats. Journal of Applied Animal Research, 51(1), 515-523. DOI: 10.1080/09712119.2023.2230754
10. Arisha, S. M. (2022): Histological, Ultrastructural, and Biochemical Investigations on Improving the Effect of Pregabalin by Flaxseed Oil on Diabetic Peripheral Neuropathy Induced in Albino Rats. Egyptian Academic Journal of Biological Sciences, D. Histology & Histochemistry, 14(2), 85-103. DOI: 10.21608/eajbsd.2022.267166.

11. Abd Ellatif, R. A., Badr, S. M., Shalaby, R. H., & Sharaf Eldin, H. E. (2023). The Role of Hesperidin in Ameliorating the Histological Changes of Sciatic Nerve in Streptozotocin-Induced Diabetic Rats: Light and Electron Microscopic Study. Egyptian Journal of Histology, 46(4), 1847-1860. DOI: 10.21608/ejh.2022.154515.1746.

12. Ibrahim, D., Abbas, F., & Howaida, S. (2024). Mechanical Allodynia and Thermal Hyperalgesia in Diabetic Mice and Neurodegenerative Changes in the Spinal Cord and Sciatic Nerves: Modulation by Topiramate. The Medical Journal of Cairo University, 91(12), 1585-1599. DOI: 10.21608/mjcu.2024.342763

13. El-Shafei, A. A., ZIckri, M. B., Mansour, S. M., El-Aziz, A., Ibrahim, M., Kareem, H. E. D. S., & Khaled, D. M. (2022): Possible Ascorbic Acid Enhanced Therapeutic Effect of Hemopoietic and Mesenchymal Stem Cells on Early Diabetic Retinopathy Rat Model: Comparative Histo-Biophysiological Study. Egyptian Journal of Histology 46(4), 1880-1892. DOI: 10.21608/ejh.2022.146693.1714.

14. Bancroft JD, and Layton C. (2019): The hematoxylin and eosin. In: Suvarna, S.K., Layton, C., Bancroft, J.D. (Eds.), Bancroft's Theory and Practice of Histological Techniques. 8th ed. ElSevier, Philadelphia, pp. 126–138. DOI: 10.1016/C2015-0-00143-5

15. Suvarna K., Layton C. and Bancroft J. (2013): Immunohistochemical techniques. In: Bancroft's Theory and practice of Histological Techniques, 7th ed. Elsevier Health Sciences, China, pp.381-426. DOI: 10.1016/B978-0-7020-4226-3.00018-4.

16. Hu, X., Agarwal, N., Zhang, M. D., Ernfors, P., Kuner, R., Nyengaard, J. R., & Karlsson, P. (2022). Identification and quantification of nociceptive Schwann cells in mice with and without Streptozotocin-induced diabetes. Journal of Chemical Neuroanatomy, 123, 102118. DOI:10.1007/s00125-023-06009-z.

17. Woods AE, Stirling JW, (2013): Transmission electron microscopy applications. In: Suvarna SK, Layton C, Bancroft JD, editors. In: Theory and Practical Histological Techniques, 7th ed. Churchill Living one, Philadelphia, pp.493 – 538. DOI:10.1016/B978-0-7020-4226 3.00022-6 .

18. Mohamady, R. E., Mohamed, M. A., & Eldahshan, A. E. (2024). The possible regenerative capability of harmine on diabetic pancreas experimentally induced by streptozotocin in adult male rats. Egyptian Journal of Histology, 47(3), 923-934. DOI: 10.21608/ejh.2023.208902.1890.

19. Abd-Elmawla, M. A., Abdelalim, E., Ahmed, K. A., & Rizk, S. M. (2023): The neuroprotective effect of pterostilbene on oxaliplatin-induced peripheral neuropathy via its anti-inflammatory, anti-oxidative and anti-apoptotic effects: Comparative study with celecoxib. Life Sciences, 315, 121364. DOI: 10.1016/j.lfs.2022.121364

20. Abdel-Tawab, N. H., Hassan, H. A., Mohamed, N. M., Hamad, N. H., & Fakhry, M. E. (2023): Effect of Quercetin on Diabetic Rat. SVU-International Journal of Medical Sciences, 6(2), 708-728. DOI: 10.21608/svuijm.2023.318230.

21. Shalaby, M. S., Abdel-Reheim, E. S., Almanaa, T. N., Alhaber, L. A., Nabil, A., Ahmed, O. M., & Abdel-Moneim, A. (2025). Therapeutic effects of mesenchymal stem cell conditioned media on streptozotocin-induced diabetes in Wistar rats. Regenerative Therapy, 28, 1-11. DOI: 10.1016/j.reth.2024.11.004.

22. Emsley R., Dunn G., &White I, (2016): Mediation and moderation of treatment effects in randomized controlled trials of complex interventions. Stat Methods Med Res, 19(3): 237–270. DOI: 10.1177/0962280209105014

23. Gopalan, H. K. (2024). Histopathological Changes in a Rat Model of Diabetic Neuropathy. Al-Anbar Journal of Veterinary Sciences, 17(1), 59-69. DOI: 10.37940/AJVS.2024.17.1.8

24. Abdel Mohsen, M. A., Ali, S. M., Salama, N. M., & Ali, E. A. (2022). Comparative histological study on the effect of erythropoietin versus curcumin on the sciatic nerve crush injury in a rat model. Egyptian Journal of Histology, 45(1), 192-207.DOI:10.21608/ejh.2021.60603.1427.

25. Abedin-Do, A., Zhang, Z., Douville, Y., Méthot, M., Bernatchez, J., & Rouabhia, M. (2022). Electrical stimulation promotes the wound-healing properties of diabetic human skin fibroblasts. Journal of Tissue Engineering and Regenerative Medicine, 16(7), 643-652. DOI:10.1093/jbmrpl/ziae155

26. Pereira, C. T., Adams, S. H., Lloyd, K. K., Knotts, T. A., James, A. W., Price, T. J., & Levi, B. (2025). Exploring the role of peripheral nerves in trauma-induced heterotopic ossification. Journal of Bone and Mineral Research, 9(1), 155. DOI: 10.1093/jbmrpl/ziae155.

27. Vaeggemose, M., Haakma, W., Pham, M., Ringgaard, S., Tankisi, H., Ejskjaer, N., & Andersen, H. (2020). Diffusion tensor imaging MR Neurography detects polyneuropathy in type 2 diabetes. Journal of Diabetes and its Complications, 34(2), 107439. DOI: 10.1016/j.jdiacomp.2019.107439

28. Sherikar, A. K., Upaganlawar, A. B., & Upasani, C. D. (2023). Effect of Topiramate on Mitochondrial Biogenesis and Neuroinflammation in Chronic Constriction Injury and Streptozotocin-induced Peripheral Neuropathy. Indian Journal of Pharmaceutical Education and Research, 57(3s), s626-s638. DOI:10.5530/ijper.57.3s.71

29. Muratori, L., Fregnan, F., Maurina, M., Haastert-Talini, K., & Ronchi, G. (2022). The Potential Benefits of Dietary Polyphenols for Peripheral Nerve Regeneration. International journal of molecular sciences, 23(9), 5177. DOI: 10.3390/ijms23095177

30. Mahmoud, H. A., El Horany, H. E., Aboalsoud, M., Abd-Ellatif, R. N., El Sheikh, A. A., & Aboalsoud, A. (2023). Targeting Oxidative Stress, Autophagy, and Apoptosis by Quercetin to Ameliorate Cisplatin-induced Peripheral Neuropathy in Rats. Journal of Microscopy and Ultrastructure, 11(2), 107-114. DOI:10.4103/jmau.jmau_78_22

31. Chen, Q. W., Meng, R. T., & Ko, C. Y. (2024). Modulating oxidative stress and neurogenic inflammation: the role of topiramate in migraine treatment. Frontiers in Aging Neuroscience, 16, 1455858. DOI: 10.3389/fnagi.2024.1455858

32. Wang, Y., Gao, B., Chen, X., Shi, X., Li, S., Zhang, Q., & Piao, F. (2024). Improvement of diabetes-induced spinal cord axon injury with taurine via nerve growth factor-dependent Akt/mTOR pathway. Amino Acids, 56(1), 32. DOI: 10.1007/s00726-023-03354-y

33. Hsueh, Y. S., Chen, S. H., Tseng, W. L., Lin, S. C., Chen, D. Q., Huang, C. C., & Hsueh, Y. Y. (2025). Leptin deficiency leads to nerve degeneration and impairs axon remyelination by inducing Schwann cell apoptosis and demyelination in type 2 diabetic peripheral neuropathy in rats. NeurochemistryInternational, 182, 105908. DOI: 10.1016/j.neuint.2024.105908

34. Bayoumi, H., Elgendy, E., Manawy, S. M., & M Kamal, K. (2024). Synergistic Effect of Vitamin B12 and Mesenchymal Stem Cells to Alleviate Paclitaxel-Induced Sciatic Neuropathy in Albino Rats Via Downregulation of NLRP3 Inflammasome Pathway: Histological and Immunohistochemical Study. Egyptian Journal of Histology, 47(2), 865-885.DOI: 10.21608/ejh.2023.293737.2026

35. Song, W., Li, Y., Jia, Y., Xu, L., Kang, L., Yang, Y., & Wu, Q. (2024). Quercetin Alleviates Diabetic Peripheral Neuropathy by Regulating Axon Guidance Factors and Inhibiting the Rho/ROCK Pathway in *vivo* and in vitro. Diabetes, Metabolic Syndrome and Obesity, 4339-4354. DOI: 10.2147/DMSO.S412955.

36. Mohammad, H. M., Eladl, M. A., Abdelmaogood, A. K., Elshaer, R. E., Ghanam, W., Elaskary, A., & Atteya, H. (2023). Protective effect of topiramate against diabetic retinopathy and computational approach recognizing the role of NLRP3/IL-1β/TNF-α signaling. Biomedicines, 11(12), 3202.DOI:10.3390/biomedicines11123202

37. Elhessy, H. M., Habotta, O. A., Eldesoqui, M., Elsaed, W. M., Soliman, M. F., Sewilam, H. M., & Lashine, N. H. (2023). Comparative neuroprotective effects of Cerebrolysin, dexamethasone, and ascorbic acid on sciatic nerve injury model: behavioral and histopathological study. Frontiers in Neuroanatomy, 17, 1090738. DOI: 10.3389/fnana.2023.1090738

38. Amin, D. M., Abaza, M., & Ibrahim, N. (2024). Alhagi maurorum Ethanolic Extract can halt potential topiramate neurotoxicity on sciatic nerve of adult male albino rats. Zagazig University Medical Journal, 30(8.1), 4241-4253. DOI: https://doi.org/10.21608/zumj.2024.324854.3606.

39. Li, J., Guan, R., & Pan, L. (2023). Mechanism of Schwann cells in diabetic peripheral neuropathy: A review. Medicine, 102(1), e32653. DOI:

40. Cheng, Y., Chen, Y., Li, K., Liu, S., Pang, C., Gao, L., & Deng, B. (2024). How inflammation dictates diabetic peripheral neuropathy: An enlightening review. CNS Neuroscience & Therapeutics, 30(4), e14477. DOI:10.1111/cns.14477.

41. Fideles, S. O. M., de Cássia Ortiz, A., Buchaim, D. V., de Souza Bastos Mazuqueli Pereira, E., Parreira, M. J. B. M., de Oliveira Rossi, J., & Buchaim, R. L. (2023). Influence of the neuroprotective properties of quercetin on regeneration and functional recovery of the nervous system. Antioxidants, 12(1), 149. DOI: 10.3390/ijms241814836.

42. Nashtahosseini, Z., Eslami, M., Paraandavaji, E., Haraj, A., Dowlat, B. F., Hosseinzadeh, E., ... & Naderian, R. (2025). Cytokine Signaling in Diabetic Neuropathy: A Key Player in Peripheral Nerve Damage. Biomedicines, 13(3), 589. DOI:10.3390/biomedicines13030589

43. Ou, X., Wang, Z., Yu, D., Guo, W., Zvyagin, A. V., Lin, Q., & Qu, W. (2025). VEGF-loaded ROS-responsive nanodots improve the structure and function of sciatic nerve lesions in type II diabetic peripheral neuropathy. Biomaterials, 315, 122906. DOI:10.1016/j.biomaterials.2024.122906

44. Mohos, V., Harmat, M., Kun, J., Aczél, T., Zsidó, B. Z., Kitka, T., & Helyes, Z. (2024). Topiramate inhibits adjuvant-induced chronic orofacial inflammatory allodynia in the rat. Frontiers in Pharmacology, 15, 1461355. DOI: 10.3389/fphar.2024.1461355

الملخص العربى

دراسة هستولوجية و كميائيه حيويه مقارنة بين تأثير الكيرسيتين و توبيراميت علي إعتلال العصب الطرفي السكري المستحدث فى ذكورالجرذان البيضاء البالغه

مي أمين المعتصم، عزة صالح معوض امبابى، سلوي خالد مصطفي إبراهيم، اسماء محمود مصطفي، فاطمه الزهراء محمد عبداللطيف

قسم الهستولوجيا الطبيه وبيولوجيا الخليه، كلية الطب، جامعه بنى سويف

المقدمة: يُعتبر اعتلال العصب الطرفي السكري من المضاعفات الشائعة لمرض السكري، مما يزيد من مخاطر البتر والوفيات إذا تُرك دون علاج. تنشأ هذه الحالة نتيجة ارتفاع مستوى السكر في الدم لفترات طويلة، مما يؤدي إلى تلف الأعصاب ووظيفتها.

هدف العمل: تهدف هذه الدراسة إلى تقييم تأثير الكيرسيتين والتوبيراميت في تخفيف الاعتلال العصبي السكري المستحدث في نماذج الجرذان.

المواد والطرق: تم استخدام خمسون جرذا أبيض بالغاً من الذكور، وتم تقسيمها إلى مجموعة ضابطة (n=١٠) ومجموعة تجريبية II) ؛ (n=٤٠ تلقت حقنة ألوكسن (١٥٠ ملغ/كغ، عن طريق الحقن في الصفاق) لتحفيز السكري. بعد أربعة أسابيع، تم تقسيم الجرذان المصابة بالسكري إلى أربع مجموعات فرعية:

- المجموعة الفرعية٢أ: بدون علاج (تحكم).
- المجموعة الفرعية ٢ب: تلقت الكيرسيتين (١٠٠ ملغ/كغ) عن طريق التغذية الفموية.
- المجموعة الفرعية ٢ج: عولجت بالتوبيراميت ا (٣٠ ملغ/كغ) عن طريق التغذية الفموية.
- المجموعة الفرعية٢د: تلقت الكيرسيتين والتوبيراميت بنفس الجرعات كما في ٢ب و٢ج

استمرت جميع العلاجات لمدة أربعة أسابيع أخرى. تم جمع عينات الدم لإجراء تقييمات كيميائية حيوية، وتم جمع الأعصاب الطرفيه لإجراء تحليل نسيجي باستخدام صبغة الهيماتوكسيلاين والإيوزين (H&E)، وصبغة التوليدين الزرقاء، والصبغة المناعية الكيميائية للكاسبيز-٣ وS-١٠٠ . تم فحص المقاطع الرقيقه باستخدام المجهر الإلكتروني، تلاها دراسات مورفومترية وإحصائية.

النتائج: أظهرت المجموعة الفرعية ٢أ تغييرات كيميائية حيوية ونسيجية ملحوظة، تمثلت في انخفاض كبير في عدد الألياف العصبية، وعدم انتظام الهياكل، وتغيرات غير طبيعية في الميالين، وزيادة في تفاعل الكاسبيز-٣. أظهرت المجموعتان الفرعيتان ٢ب و ٢ج تحسن مماثل، وإن كانت جزئية. ومن الجدير بالذكر أن المجموعة الفرعية ٢د أظهرت نتائج تجديدية مثالية، مما يدل على أن العلاج المشترك يعزز بشكل كبير من إصلاح الأعصاب مقارنة بالعلاجات الفردية.

الخلاصة: يوفر الاستخدام المتزامن للكيرسيتين والتوبيرميت تأثيرات تجديدية أفضل في الاعتلال العصبي السكري المحفز تجريبياً مقارنةً بأي من العلاجات بمفردها، مما يبرز إمكانات استراتيجيات العلاج المركبة في إدارة الالتهاب العصبي السكري.